Classical Collisions

Elastic and Inelastic

INELASTIC

$P: \quad p_1 + p_2 = p_1' + p_2'$

$$m_1 v_1 + m_2 v_2 = m_1 v_1' + m_2 v_2'$$

$$v_1' = v_2' = v$$

$m_1 \qquad m_2$

1 EQUATION
1 UNKNOWN

$P: \quad m_1 v_1$

$M: \quad m_1 + m_2 = m_3$

$E: \quad \frac{1}{2} m_1 v_1^2$

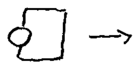

$P: \quad (m_1 + m_2)\, v$

$E: \quad \frac{1}{2} (m_1 + m_2)\, v^2$

$P: \quad m_1 v_1 = (m_1 + m_2)\, v$

$$v = \frac{m_1}{(m_1 + m_2)} v_1$$

$E: \quad \Delta E = \frac{1}{2} m_1 v_1^2 - \frac{1}{2} (m_1 + m_2)\, v^2$

$$v^2 = \frac{m_1^2}{(m_1 + m_2)^2} v_1^2$$

$$\Delta E = \frac{1}{2} \left(m_1 - \frac{m_1^2}{(m_1 + m_2)} \right) v_1^2$$

ELASTIC

m_1 $\qquad\qquad$ m_2

p: $m_1 v_1$

E: $\frac{1}{2} m_1 v_1^2$

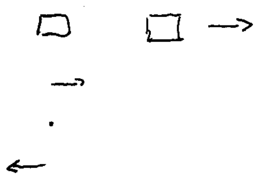

p: $m_1 v_1' + m_2 v_2'$

E: $\frac{1}{2} m_1 (v_1')^2 + \frac{1}{2} m_2 (v_2')^2$

p: $m_1 v_1 = m_1 (v_1') + m_2 (v_2')$

E $\frac{1}{2} m_1 v_1^2 = \frac{1}{2} m_1 (v_1')^2 + \frac{1}{2} m_2 (v_2')^2$

p: $m_1 v_1 + m_2 v_2 = m_1 v_1' + m_2 v_2'$

: $p_1 + p_2 = p_1' + p_2'$

E: $\frac{1}{2} m_1 v_1^2 + \frac{1}{2} m_2 v_2^2 = \frac{1}{2} m_1 (v_1')^2 + \frac{1}{2} m_2 (v_2')^2$

M: $m_1' = m_1$

$m_2' = m_2$

$m_1 + m_2 = m_1' + m_2'$

2 EQUATIONS

2 UNKNOWNS

p : $m_1 \vec{v}_1 + m_2 \vec{v}_2 = m_1 \vec{v}_1' + m_2 \vec{v}_2'$

E : $\frac{1}{2} m_1 v_1^2 + \frac{1}{2} m_2 v_2^2 = \frac{1}{2} m_1 (v_1')^2 + \frac{1}{2} m_2 (v_2')^2$

m : $m_1 + m_2$ CONSTANT

The coefficient of restitution

Energy in Collisions

c.o.r.	type	total kinetic energy	comments
0	perfectly inelastic	decreases to a minimum	objects stick together
~ 0	inelastic	decreases by any amount	all collisions between macroscopic bodies, high energy collisions between subatomic particles
~ 1	partially elastic or nearly elastic	"nearly conserved"	billiard balls, bowling balls, steel bearings and other objects made from resilient materials
1	elastic	absolutely conserved	low energy collisions between atoms, molecules, subatomic particles
> 1	superelastic	increases	contrived collisions between objects that release potential energy on contact, fictional superelastic materials like flubber

The coefficient of restitution

Equation

[edit]

Picture a one-dimensional collision. Velocity in an arbitrary direction is labeled "positive" and the opposite direction "negative".

The coefficient of restitution is given by

$$C_R = \frac{v_b - v_a}{u_a - u_b}$$

for two colliding objects, where

v_a is the final velocity of the first object after impact

v_b is the final velocity of the second object after impact

u_a is the initial velocity of the first object before impact

u_b is the initial velocity of the second object before impact

Even though the equation does not reference mass, it is important to note that it still relates to momentum since the final velocities are dependent on mass.

For an object bouncing off a stationary object, such as a floor:

$$C_R = \frac{v}{u}, \text{ where}$$

v is the scalar velocity of the object after impact

u is the scalar velocity of the object before impact

The coefficient of restitution

Speeds after impact

[edit]

The equations for collisions between elastic particles can be modified to use the COR, thus becoming applicable to inelastic collisions as well, and every possibility in between.

$$v_a = \frac{m_a u_a + m_b u_b + m_b C_R (u_b - u_a)}{m_a + m_b}$$

and

$$v_b = \frac{m_a u_a + m_b u_b + m_a C_R (u_a - u_b)}{m_a + m_b}$$

where

- v_a is the final velocity of the first object after impact
- v_b is the final velocity of the second object after impact
- u_a is the initial velocity of the first object before impact
- u_b is the initial velocity of the second object before impact
- m_a is the mass of the first object
- m_b is the mass of the second object

The coefficient of restitution

Sports equipment

[edit]

The coefficient of restitution entered the common vocabulary, among golfers at least, when golf club manufacturers began making thin-faced drivers with a so-called "trampoline effect" that creates drives of a greater distance as a result of an extra bounce off the clubface. The USGA (America's governing golfing body) has started testing drivers for COR and has placed the upper limit at 0.83, golf balls typically have a COR of about 0.78.[6] According to one article (addressing COR in tennis racquets), "[f]or the Benchmark Conditions, the coefficient of restitution used is 0.85 for all racquets, eliminating the variables of string tension and frame stiffness which could add or subtract from the coefficient of restitution."[7]

The International Table Tennis Federation specifies that the ball must have a coefficient of restitution of 0.94.[8]

The coefficient of restitution

object	H (cm)	h_1 (cm)	h_2 (cm)	h_3 (cm)	h_4 (cm)	h_5 (cm)	h_{ave} (cm)	c.o.r.
range golf ball	92	67	66	68	68	70	67.8	0.858
tennis ball	92	47	46	45	48	47	46.6	0.712
billiard ball	92	60	55	61	59	62	59.4	0.804
hand ball	92	51	51	52	53	53	52.0	0.752
wooden ball	92	31	38	36	32	30	33.4	0.603
steel ball bearing	92	32	33	34	32	33	32.8	0.597
glass marble	92	37	40	43	39	40	39.8	0.658
ball of rubber bands	92	62	63	64	62	64	63.0	0.828
hollow, hard plastic ball	92	47	44	43	42	42	43.6	0.688

Classical 1d elastic collisions

One-dimensional Newtonian

[edit]

Consider two particles, denoted by subscripts 1 and 2. Let m_i be the masses, u_i the velocities before collision and v_i the velocities after collision.

The conservation of the total momentum demands that the total momentum before the collision is the same as the total momentum after the collision, and is expressed by the equation

$$m_1 u_1 + m_2 u_2 = m_1 v_1 + m_2 v_2.$$

Likewise, the conservation of the total kinetic energy is expressed by the equation

$$\frac{m_1 u_1^2}{2} + \frac{m_2 u_2^2}{2} = \frac{m_1 v_1^2}{2} + \frac{m_2 v_2^2}{2}.$$

These equations may be solved directly to find v_i when u_i are known or vice versa. However, the algebra[1] can get messy. A cleaner solution is to first change the frame of reference such that one of the known velocities is zero. The unknown velocities in the new frame of reference can then be determined and followed by a conversion back to the original frame of reference to reach the same result. Once one of the unknown velocities is determined, the other can be found by symmetry.

Solving these simultaneous equations for v_i we get:

$$v_1 = \frac{u_1(m_1 - m_2) + 2m_2 u_2}{m_1 + m_2}, v_2 = \frac{u_2(m_2 - m_1) + 2m_1 u_1}{m_1 + m_2}$$

OR

$$v_1 = u_1, v_2 = u_2.$$

Classical 1d elastic collisions in the center of momentum frame

Classical Mechanics is only a good approximation. It will give accurate results when it deals with the object which is macroscopic and running with much lower speed than the speed of light. Beyond the classical limits, it will give a wrong result. Total momentum of the two colliding bodies is frame-dependent. In the center of momentum frame, according to Classical Mechanics,

$$m_1 u_1 + m_2 u_2 = m_1 v_1 + m_2 v_2 = 0$$
$$m_1 u_1^2 + m_2 u_2^2 = m_1 v_1^2 + m_2 v_2^2$$
$$\frac{(m_2 u_2)^2}{2m_1} + \frac{(m_2 u_2)^2}{2m_2} = \frac{(m_2 v_2)^2}{2m_1} + \frac{(m_2 v_2)^2}{2m_2}$$
$$(m_1 + m_2)(m_2 u_2)^2 = (m_1 + m_2)(m_2 v_2)^2$$

=> $u_2 = -v_2$

$$\frac{(m_1 u_1)^2}{2m_1} + \frac{(m_1 u_1)^2}{2m_2} = \frac{(m_1 v_1)^2}{2m_1} + \frac{(m_1 v_1)^2}{2m_2}$$
$$(m_1 + m_2)(m_1 u_1)^2 = (m_1 + m_2)(m_1 v_1)^2$$

=> $u_1 = -v_1$

Classical 2d elastic collisions in the center of momentum frame

In a center of momentum frame at any time the velocities of the two bodies are in opposite directions, with magnitudes inversely proportional to the masses. In an elastic collision these magnitudes do not change. The directions may change depending on the shapes of the bodies and the point of impact. For example, in the case of spheres the angle depends on the distance between the (parallel) paths of the centers of the two bodies. Any non-zero change of direction is possible: if this distance is zero the velocities are reversed in the collision; if it is close to the sum of the radii of the spheres the two bodies are only slightly deflected.

Assuming that the second particle is at rest before the collision, the angles of deflection of the two particles, ϑ_1 and ϑ_2, are related to the angle of deflection θ in the system of the center of mass by [2]

$$\tan\vartheta_1 = \frac{m_2 \sin\theta}{m_1 + m_2\cos\theta}, \qquad \vartheta_2 = \frac{\pi}{2} - \theta.$$

The velocities of the particles after the collision are:

$$v'_1 = v_1 \frac{\sqrt{m_1^2 + m_2^2 + 2m_1 m_2 \cos\theta}}{m_1 + m_2}, \qquad v'_2 = v_1 \frac{2m_1}{m_1 + m_2} \sin\frac{\theta}{2}.$$

Collision Applets

https://www.msu.edu/~brechtjo/physics/airTrack/airTrack.html

http://surendranath.org/Applets/Dynamics/Collisions/CollisionApplet.html

http://galileoandeinstein.physics.virginia.edu/more_stuff/Applets/Collision/jarapplet.html

http://burro.cwru.edu/JavaLab/GalCrashWeb/

http://demonstrations.wolfram.com/ElasticCollisionsOfTwoSpheres/

http://demonstrations.wolfram.com/InelasticCollisionsOfTwoSpheres/

http://demonstrations.wolfram.com/InelasticCollisionsOfTwoRoughSpheres/

Relativistic 1d Elastic Collisions in the Center of Momentum Frame

One-dimensional relativistic

[edit]

According to Special Relativity,

$$p = \frac{mv}{\sqrt{1 - \frac{v^2}{c^2}}}$$

Where p denotes momentum of any massive particle, v denotes velocity, c denotes the speed of light.

in the center of momentum frame where the total momentum equals zero,

$$p_1 = - p_2$$

$$p_1^2 = p_2^2$$

$$\sqrt{m_1^2c^4 + p_1^2c^2} + \sqrt{m_2^2c^4 + p_2^2c^2} = E$$

$$p_1 = \pm \frac{\sqrt{E^4 - 2E^2m_1^2c^4 - 2E^2m_2^2c^4 + m_1^4c^8 - 2m_1^2m_2^2c^8 + m_2^4c^8}}{cE}$$

$$u_1 = - v_1$$

It is shown that $u_1 = -v_1$ remains true in relativistic calculation despite other differences. One of the postulates in Special Relativity states that the Laws of Physics should be invariant in all inertial frames of reference. That is, if total momentum is conserved in a particular inertial frame of reference, total momentum will also be conserved in any inertial frame of reference, although the amount of total momentum is frame-dependent. Therefore, by transforming from an inertial frame of reference to another, we will be able to get the desired results. In a particular frame of reference where the total momentum could be any,

$$\frac{m_1\, u_1}{\sqrt{1-u_1^2/c^2}}+\frac{m_2\, u_2}{\sqrt{1-u_2^2/c^2}}=\frac{m_1\, v_1}{\sqrt{1-v_1^2/c^2}}+\frac{m_2\, v_2}{\sqrt{1-v_2^2/c^2}}=p_T$$
$$\frac{m_1 c^2}{\sqrt{1-u_1^2/c^2}}+\frac{m_2 c^2}{\sqrt{1-u_2^2/c^2}}=\frac{m_1 c^2}{\sqrt{1-v_1^2/c^2}}+\frac{m_2 c^2}{\sqrt{1-v_2^2/c^2}}=E$$

We can look at the two moving bodies as one system of which the total momentum is p_T, the total energy is E and its velocity v_c is the velocity of its center of mass. Relative to the center of momentum frame the total momentum equals zero. It can be shown that v_c is given by:

$$v_c = \frac{p_T c^2}{E}$$

Now the velocities before the collision in the center of momentum frame u_1' and u_2' are:

$$u_1' = \frac{u_1 - v_c}{1-\frac{u_1 v_c}{c^2}}$$
$$u_2' = \frac{u_2 - v_c}{1-\frac{u_2 v_c}{c^2}}$$
$$v_1' = -u_1'$$
$$v_2' = -u_2'$$
$$v_1 = \frac{v_1' + v_c}{1+\frac{v_1' v_c}{c^2}}$$
$$v_2 = \frac{v_2' + v_c}{1+\frac{v_2' v_c}{c^2}}$$

When $u_1 << c$ and $u_2 << c$,

Momentum in relativistic mechanics

[edit]

In relativistic mechanics, in order to be conserved, the momentum of an object must be defined as

$$\mathbf{p} = \gamma m_0 \mathbf{v}\,,$$

where m_0 is the invariant mass of the object and γ is the Lorentz factor, given by

$$\gamma = \frac{1}{\sqrt{1-(v/c)^2}}\,,$$

where v is the speed of the object and c is the speed of light. The inverse relation is given by:[15]

$$\mathbf{v} = \frac{c^2\mathbf{p}}{\sqrt{(pc)^2+(m_0c^2)^2}} = \frac{c^2\mathbf{p}}{E}\,,$$

where $p = \sqrt{p_x^2+p_y^2+p_z^2}$ is the magnitude of the momentum.

Relativistic momentum can also be written as invariant mass times the object's proper velocity, defined as the rate of change of object position in the observer frame with respect to time elapsed on object clocks (i.e. object proper time). Within the domain of classical mechanics, relativistic momentum closely approximates Newtonian momentum: at low velocity, $\gamma m_0\mathbf{v}$ is approximately equal to $m_0\mathbf{v}$, the Newtonian expression for momentum.

The total energy E of a body is related to the relativistic momentum **p** by

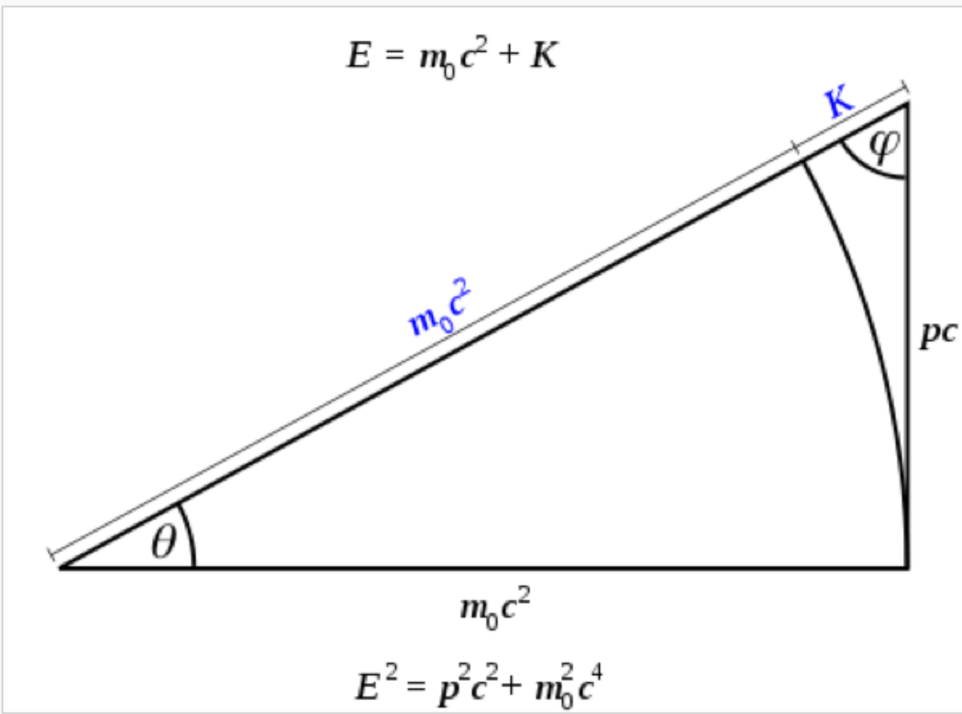

A graphical representation of the interrelation of relativistic energy E, invariant mass m_0, relativistic momentum p, and relativistic mass $m = \gamma m_0$.

$$E^2 = (pc)^2 + (m_0c^2)^2\,,$$

where p denotes the magnitude of **p**. This relativistic energy-momentum relationship holds even for massless particles such as photons; by setting $m_0 = 0$ it follows that

$$E = pc\,.$$

For both massive and massless objects, relativistic momentum is related to the de Broglie wavelength λ by

$$p = h/\lambda\,,$$

where h is the Planck constant.

Four-vector formulation

[edit]

Relativistic four-momentum as proposed by Albert Einstein arises from the invariance of four-vectors under Lorentzian translation. The four-momentum **P** is defined as:

$$\mathbf{P} := (E/c, p_x, p_y, p_z)\,,$$

where $E = \gamma m_0 c^2$ is the total relativistic energy of the system, and p_x, p_y, and p_z represent the *x*-, *y*-, and *z*-components of the relativistic momentum, respectively.

The magnitude ||**P**|| of the momentum four-vector is equal to $m_0 c$, since

$$||\mathbf{P}||^2 = (E/c)^2 - p^2 = (m_0 c)^2\,.$$

which is invariant across all reference frames. For a closed system, the total four-momentum is conserved, which effectively combines the conservation of both momentum and energy into a single equation. For example, in the radiationless collision of two particles with rest masses m_1 and m_2 with initial velocities $\mathbf{v}_1$ and $\mathbf{v}_2$, the respective final velocities $\mathbf{v}_3$ and $\mathbf{v}_4$ may be found from the conservation of four-momentum which states that:

$$\mathbf{P}_1 + \mathbf{P}_2 = \mathbf{P}_3 + \mathbf{P}_4\,,$$

where

$$\mathbf{P}_i = m_i \gamma_i (c, \mathbf{v}_i).$$

For elastic collisions, the rest masses remain the same ($m_1 = m_3$ and $m_2 = m_4$), while for inelastic collisions, the rest masses will increase after collision due to an increase in their heat energy content. The conservation of four-momentum can be shown to be the result of the homogeneity of space–time.

Generalization of momentum

[edit]

Momentum is the Noether charge of translational invariance. As such, not just particles, but fields and other things can have momentum. However, where space–time is curved there is no Noether charge for translational invariance.

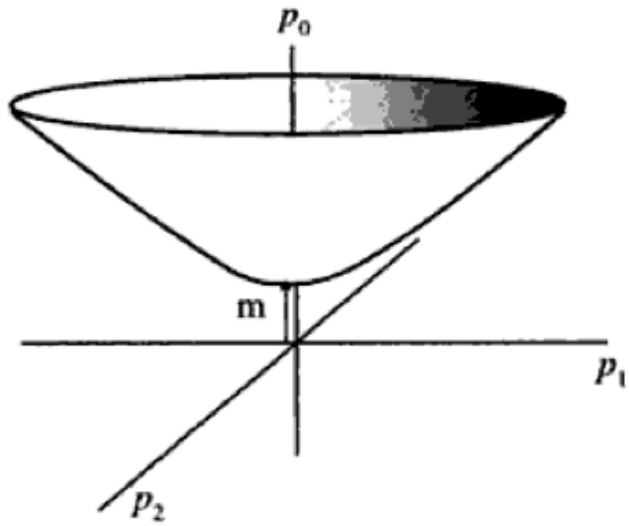

Figure 3.3. Finite mass hyperbola.

Mass

Sheels

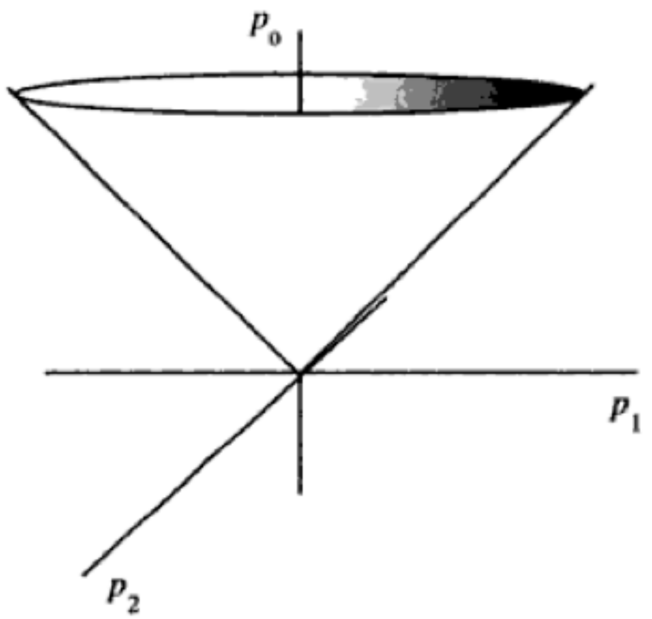

Figure 3.4. Zero mass hyperbola.

mass zero. Their mass hyperbola is the cone depicted in Figure 3.4. Conversely, particles with zero invariant mass travel with the speed of light. One can easily show (see Exercise 1) that, if the four-momenta of two particles are added (i.e., if the corresponding components are added to obtain the components of the sum), the resulting four-momentum is timelike, the invariant being greater than zero, or light like, the invariant being zero. It is lightlike only if the two original four-momentum vectors are themselves lightlike, with their space momenta parallel. It follows that in adding the four-momenta of any number of particles, one always obtains a timelike four-vector (unless, of course, all the particles' four-momenta that are added are lightlike with all three-momentum vectors parallel). This four-momentum has does not "soft land," that is, we assume that $y'(T(\theta)) < 0$, where $T(\theta)$ is the impact time. From (2) and the definitions of f_2 and f_4, we have

$$y'(t)=v \sin \theta f_2'(t)-gf_4'(t)=e^{-f_1(t)}(v \sin \theta - gf_3(t))$$

and hence the impact assumption is

$$f_3(T(\theta))>\frac{v}{g} \sin \theta. \tag{9}$$

In terms of the function

$$\rho(\theta)=\frac{R(\theta)}{v \cos \theta}$$

we have by (1),

$$R(\theta)=x(T(\theta))=v \cos \theta f_2(T(\theta))$$

and hence

$$T(\theta)=f_2^{-1}(\rho(\theta)).$$

The impact assumption (9) is therefore equivalent to

$$f_3(f_2^{-1}(\rho(\theta)))>\frac{v}{g} \sin \theta. \tag{10}$$

Now, $R(\theta)$ is differentiable if and only if $\rho(\theta)$ is differentiable. By (3), $\rho(\theta)$ is defined by $P(\rho(\theta), \theta)=0$, where

$$P(\rho,\theta)=v \sin \theta\rho - gf_4(f_2^{-1}(\rho)).$$

Finally, at $\rho = \rho(\theta)$,

$$\frac{\partial P}{\partial \rho}=v \sin \theta - gf_4'(f_2^{-1}(\rho))f_2^{-1\prime}(\rho)$$
$$=v \sin \theta - gf_3(f_2^{-1}(\rho))<0$$

by (10), and hence $\rho(\theta)$ is differentiable by the Implicit Function Theorem.[7]

[1]G. Galilei, *Two New Sciences* (Elzevirs, Leyden, 1638), translated with a new introduction and notes, by Stillman Drake (Wall and Thompson, Toronto, 1989), 2nd ed., p. 245.
[2]S. Drake and I. Drabkin, *Mechanics in Sixteenth-Century Italy* (University of Wisconsin Press, Madison, 1969), p. 91.
[3]K. Symon, *Mechanics* (Addison-Wesley, Reading, MA, 1953), p. 38.
[4]H. Erlichson, "Maximum projectile range with drag and lift, with particular application to golf," Am. J. Phys. **51**, 357–361 (1983).
[5]T. de Alwis, "Projectile motion with arbitrary resistance," Coll. Math. J. **26**, 361–366 (1995).
[6]J. Lekner, "What goes up must come down; will air resistance make it return sooner, or later?," Math. Mag. **55**, 26–28 (1982).
[7]R. Courant, *Differential and Integral Calculus* (Interscience, New York, 1961), Vol. II, p. 114.

Minkowski diagrams in momentum space

Eugene J. Saletan
Physics Department, Northeasten University, Boston, Massachusetts 02115

(Received 3 February 1997; accepted 12 February 1997)

I. INTRODUCTION

Minkowski diagrams in configuration space, with points representing events, are often used in undergraduate courses on special relativity. Similar diagrams in momentum space are seldom shown, and the object of this note is to demonstrate their pedagogical usefulness in discussing particle interactions. In configuration space each point has coordinates $(t,\mathbf{x})$; in momentum space the coordinates are $(E,\mathbf{p})$. Two examples should be sufficient to show how such diagrams can be used.

II. EXAMPLES

A. Fission

In this example there is just one space dimension: Minkowski space is two dimensional. A particle of mass m is represented by its mass shell, a hyperbola opening in the positive E direction, given by

$$\left(\frac{E}{c}\right)^2 - p^2=(mc)^2.$$

Figure 1 shows two such mass shells belonging to masses m and $M>m$, each labeled by its mass. The scale on the energy axis is chosen as E/c rather than E, so the two mass shells cross the E/c axis at mc and Mc, respectively. Each point on an m mass shell represents a state of a particle of mass m, i.e., possible values of its energy and momentum. A vector from the origin to such a point represents the energy–momentum $(E-p)$ vector of that state.

Consider a particle of mass M at rest, say a uranium nucleus, that undergoes fission to two particles of equal mass m. The vertical arrow in Fig. 1 represents the original uranium $E-p$ vector. $E-p$ conservation implies that the $E-p$ vectors of the two fission fragments add up to the original one, and since the total momentum is zero, the momenta of the two fission fragments must be negatives: their $E-p$ vectors have opposite p components. Symmetry of the m mass shell about the E/c axis then implies that their E/c components are equal, and conservation then implies than each E/c component is equal to $Mc/2$. It is clear from the dia-

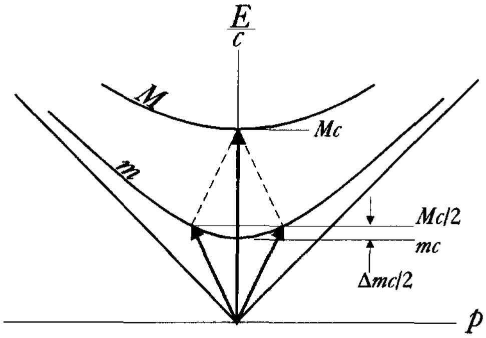

Fig. 1. Fission.

gram that each E/c component is higher than the point at which the m mass shell crosses the E/c axis, i.e., greater than mc, so $m<\frac{1}{2}M$,

$$Mc-2mc\equiv\Delta mc>0.$$

As the fission fragments interact with their surroundings, they slow down and eventually come to rest. Then their total E/c is $2mc$, so the energy they give up to their surroundings is just $\Delta E=\Delta mc^2$. This is the real content of the famous equation $E=mc^2$, involving measurable energy changes rather than absolute values relative to some more or less arbitrarily chosen zero of energy. Note that the mass of the fission fragments is not determined. But because their energies are both $\frac{1}{2}Mc^2$, the mass m and momentum p are related by

$$\left(\tfrac{1}{2}Mc\right)^2-p^2=(mc)^2.$$

The logical order in which to present this in class is first to draw the M mass shell, then the two $E-p$ vectors of the fission fragments, and only then to draw in the m mass shell.

This example is easily generalized to fission fragments of unequal masses. Also, a similar diagram can be used to illustrate fusion or the binding energy of the deuteron. Then M is less than $2m$, and the M mass shell crosses the E/c axis below $2mc$.

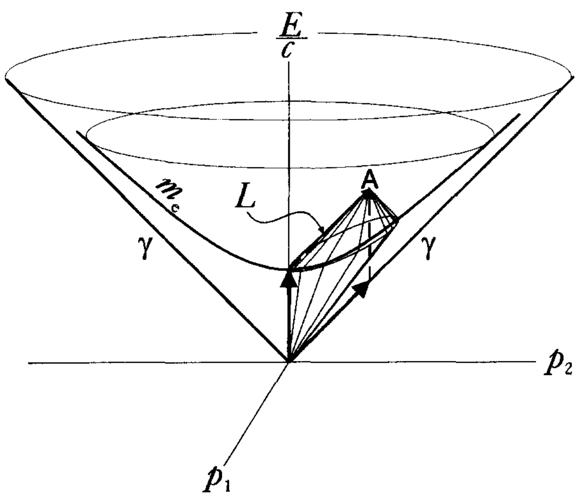

Fig. 2. Compton scattering.

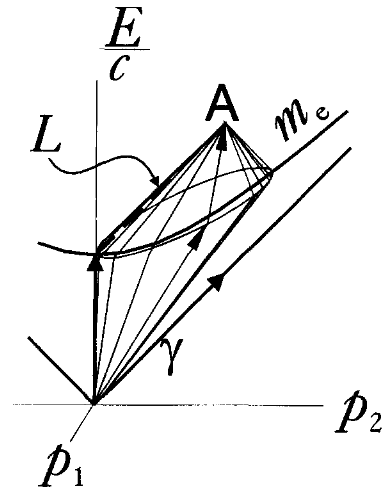

Fig. 3. Compton scattering (detail).

B. Compton scattering

Now take Minkowski space to be three dimensional, as in Fig. 2. The mass shell is now a hyperboloid of revolution. In the figure the intersection of the $(E/c,p_2)$ plane with the electron mass shell is the hyperbola labeled m_e, and the intersection with the light cone consists of the two lines labeled γ. The light cone is the mass shell of the photon, whose equation is

$$\left(\frac{E}{c}\right)^2-|\mathbf{p}|^2=0.$$

The vertical arrow in Fig. 2 is the $E-p$ vector of an electron at rest, and the other arrow represents an incident photon. The system's total $E-p$ vector is represented by the point labeled A (the vector to A is not drawn to avoid confusion). After scattering, the electron $E-p$ vector (again on the electron mass shell) plus the scattered photon $E-p$ vector (again on the light cone) must add up to A. A way to draw this is to construct an inverted light cone L with its vertex at A. The $E-p$ vectors of all possible scattered photons arrive at A from the closed curve, almost a circle, at which L intersects m_e in this three-dimensional space–time (in four dimensions this would be a closed surface, almost a sphere).

Figure 3 is an enlargement of part of Fig. 2. One possible combination of scattered electron and photon $E-p$ vectors is indicated with arrows. The direction of the scattered photon is obtained by projecting its $E-p$ vector onto the (p_1,p_2) plane, so the different lines on the cone represent photons moving in different directions. It is immediately evident that the photon energy E, and hence its frequency ν and wavelength λ, are determined by its direction.

III. CONCLUSION

Other particle interactions can also be visualized on similar Minkowski diagrams. The goal of this note is to show how the dynamics can be visualized, not to perform the calculations. The equations of the mass shells can be used, however, as a starting point for going on to the calculations.

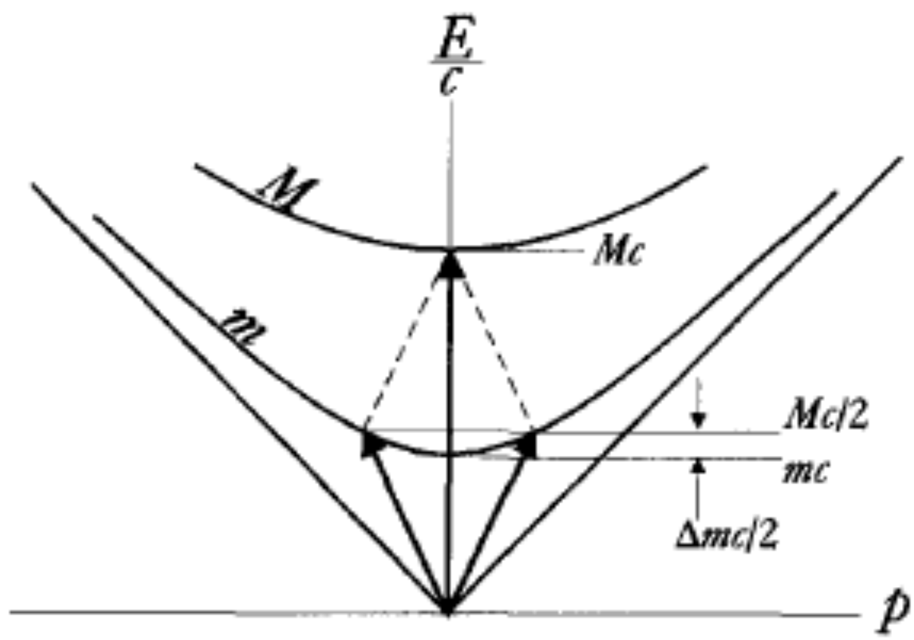

Fig. 1. Fission.

Compton Scattering Algebra

Solution

Week 69 (1/5/04)

Compton scattering

We will solve this problem by making use of 4-momenta. The *4-momentum* of a particle is given by

$$P \equiv (P_0, P_1, P_2, P_3) \equiv (E, p_x c, p_y c, p_z c) \equiv (E, \mathbf{p}c). \tag{1}$$

In general, the inner-product of two *4-vectors* is given by

$$A \cdot B \equiv A_0 B_0 - A_1 B_1 - A_2 B_2 - A_3 B_3. \tag{2}$$

The square of a 4-momentum (that is, the inner product of a 4-momentum with itself) is therefore

$$P^2 \equiv P \cdot P = E^2 - |\mathbf{p}|^2 c^2 = m^2 c^4. \tag{3}$$

Let's now apply these idea to the problem at hand. We will actually be doing nothing here other than applying conservation of energy and momentum. It's just that the language of 4-vectors makes the whole procedure surprisingly simple. Note that conservation of E and $\mathbf{p}$ during the collision can be succinctly written as

$$P_{\text{before}} = P_{\text{after}}. \tag{4}$$

Referring to the figure below, the 4-momenta before the collision are

$$P_\gamma = \left(\frac{hc}{\lambda}, \frac{hc}{\lambda}, 0, 0\right), \qquad P_m = (mc^2, 0, 0, 0). \tag{5}$$

And the 4-momenta after the collision are

$$P'_\gamma = \left(\frac{hc}{\lambda'}, \frac{hc}{\lambda'}\cos\theta, \frac{hc}{\lambda'}\sin\theta, 0\right), \qquad P'_m = (\text{we won't need this}). \tag{6}$$

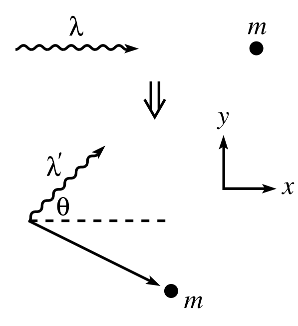

If we wanted to, we could write P'_m in terms of its momentum and scattering angle. But the nice thing about this 4-momentum method is that we don't need to introduce any quantities that we're not interested in.

Conservation of energy and momentum give $P_\gamma + P_m = P'_\gamma + P'_m$. Therefore,

$$\begin{aligned} (P_\gamma + P_m - P'_\gamma)^2 &= P'^2_m \\ \Longrightarrow P^2_\gamma + P^2_m + P'^2_\gamma + 2P_m(P_\gamma - P'_\gamma) - 2P_\gamma P'_\gamma &= P'^2_m \\ \Longrightarrow 0 + m^2c^4 + 0 + 2mc^2\left(\frac{hc}{\lambda} - \frac{hc}{\lambda'}\right) - 2\frac{hc}{\lambda}\frac{hc}{\lambda'}(1-\cos\theta) &= m^2c^4. \end{aligned} \tag{7}$$

Multiplying through by $\lambda\lambda'/(2hmc^3)$ gives the desired result,

$$\lambda' = \lambda + \frac{h}{mc}(1-\cos\theta). \tag{8}$$

The ease of this solution arose from the fact that all the unknown garbage in P'_m disappeared when we squared it.

Remarks:

1. If $\theta \approx 0$ (that is, not much scattering), then $\lambda' \approx \lambda$, as expected.
2. If $\theta = \pi$ (that is, backward scattering) and additionally $\lambda \ll h/mc$ (that is, $mc^2 \ll hc/\lambda = E_\gamma$), then $\lambda' \approx 2h/mc$, so

$$E'_\gamma = \frac{hc}{\lambda'} \approx \frac{hc}{\frac{2h}{mc}} = \frac{1}{2}mc^2. \tag{9}$$

Therefore, the photon bounces back with an essentially fixed E'_γ, independent of the initial E_γ (as long as E_γ is large enough). This isn't all that obvious.

Evening MS Projects

Independent Study Project
with a physics professor or with
a suitable* professor and topic
in another department

min 6 credits of Physics 600
max 18 credits of Physics 600

Procedure

Do your research
Write your project paper
Make your project presentation
Answer questions from your
exam committee

***Prof. Wilkes defines suitable**

Project Categories

(1) With a campus research group
physics, applied physics lab, geophysics, medical physics, biophysics, astronomy, ...

(2) Related to employer
Boeing, Synrad, Microvision, ...

(3) Related to EMS Lab classes
SPR, EPR, Chaos, The Lamb Shift, ...

(3) Related to teaching
virtual books, new labs, software

(4) Purely curiosity driven
Tokamaks, Virtual Photons, Sprinklers

Project Title	Physics Faculty Supervisor
• *Electrodynamics and Riemannian Gravitational Interaction*	*M. Baker*
• *Investigating in-service teacher, college student, and high school student conceptions of Newton's Second Law: A comparative analysis*	*L. McDermott*
• *A Computer Simulation of the X-ray Fluorescence Holographic Technique in Crystallography*	*L. Sorensen*
• *EPR Correlations in Annihilation Photon Experiments*	*L. Sorensen*
• *Measurement of Tip-Sample Forces in Tapping Atomic Force Microscopy*	*S. Fain*
• *The Effect of the Scattering Phase Shift Delta on Atomic Resolution Internal Source X-ray Holography*	*L. Sorensen*
• *Ultrasound Reflection from Specular Targets in Homogeneous and Inhomogeneous Media*	*R. Ingalls*
• *Automatic Pattern Recognition of Particle Beam Tracks using Clustering Methods and User-Interactive Mode*	*J. Wilkes*
• *Neural Networks: A Back-propagation Network for Particle Identification in a Neutrino Detector*	*J. Wilkes*
• *Chirp Sonar System Development and Testing*	*J. Wilkes*

My Recent EMSP Students

1	John Sinon	Wendy Ermold
2	Eric Herrera	Richard Hester
3	Roland Mueller	Joanne Kang
4	Larry Brandt	Dean Vestikas
5	Jeff Broderick	Nathan Horton
6	Christopher Cross	Tadd Lisman
7	David DeBruyne	Thomas Montague
8	Steven Kohlmyer	John Page
9	Gary Weber	Justin Ryser
10	Nicole Gillespie	Alin Pasca
11	Dev Sen	Charles Rust
12	Cody Young	David Wine
13	Michael Beard	Michiel Zuidweg
14	Mark Mendez	Megan Garske
15	Brian Kalab	Robert Bachilla
16	Jeremy Cooper	Rebecca Adams
17	Jin Li	Jeremy Brockman
18	Robert Moore	Eugena Pasca
19	Edwin Obune	Brian Lundstrom
20	Paul Unwin	Tom Erchul
21	Armando Lemus	Margaret Mead
22	Dennis Lewis	Roger Wolfson
23	Matthew Williams	Farid Rafla
24	Tareq Alrefae	Richard Denny

Work related research:

Boeing
Antenna Theory and Experiments
Dennis Lewis
Matthew Williams
Nathan Horton
Satellite Communications
Margaret Mead

Synrad
CO_2 Lasers
Jeff Broderick
Alin Pasca
Megan Garske

Microvision
Jenny Pasca

Improving the Optical Properties of Reflected Light for Head-up Display Applications

Independent study report

Eugenia Pasca

Diagram of the wedged HUD Windshield

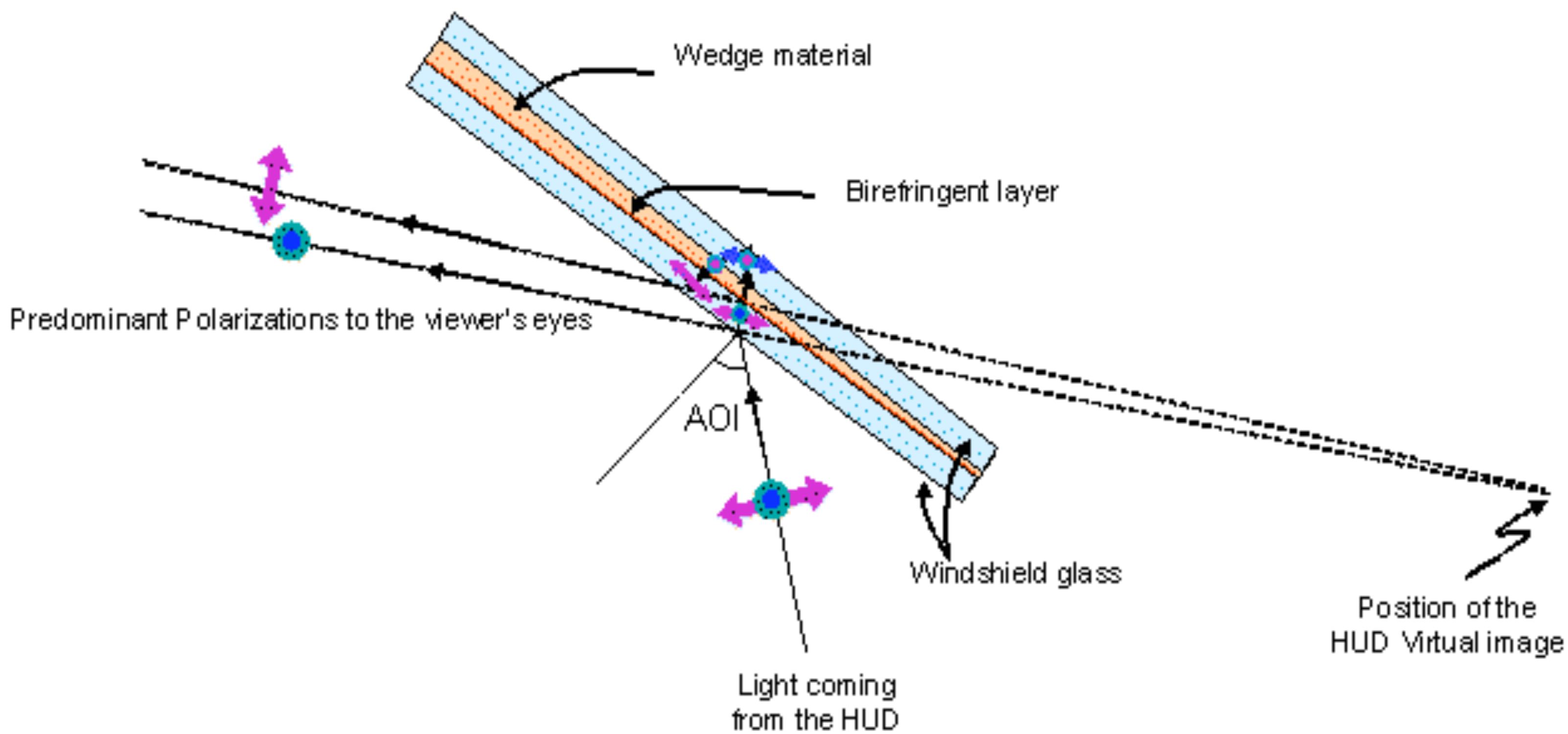

Methods to Improve Mode Discrimination and Power Stability of a Short Cavity CO_2 Laser

Dorin Marin Alin Pasca

Old 48 Series

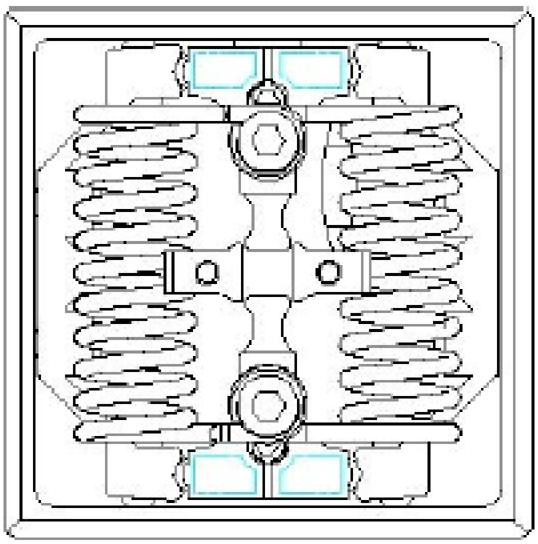

Alin's New Series

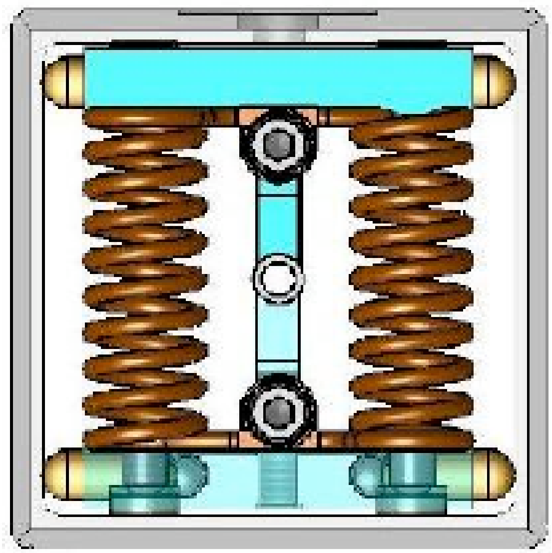

Old V Series

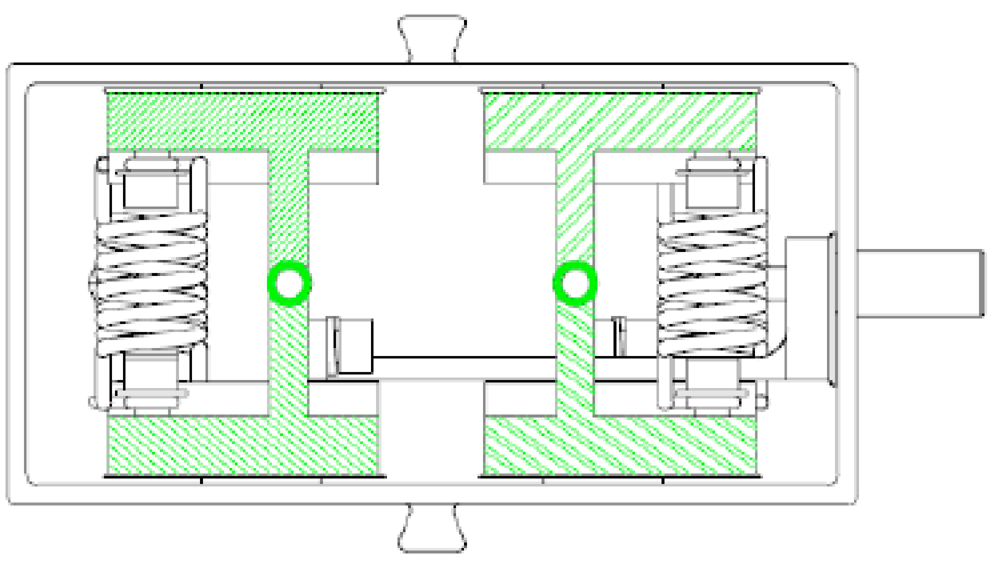

Shielding Effectiveness Evaluation of an Electrically Large, Complex Cavity Using Various Mode-stir Measurements and Numerical Calculations

Nathan Horton

June 7, 2005

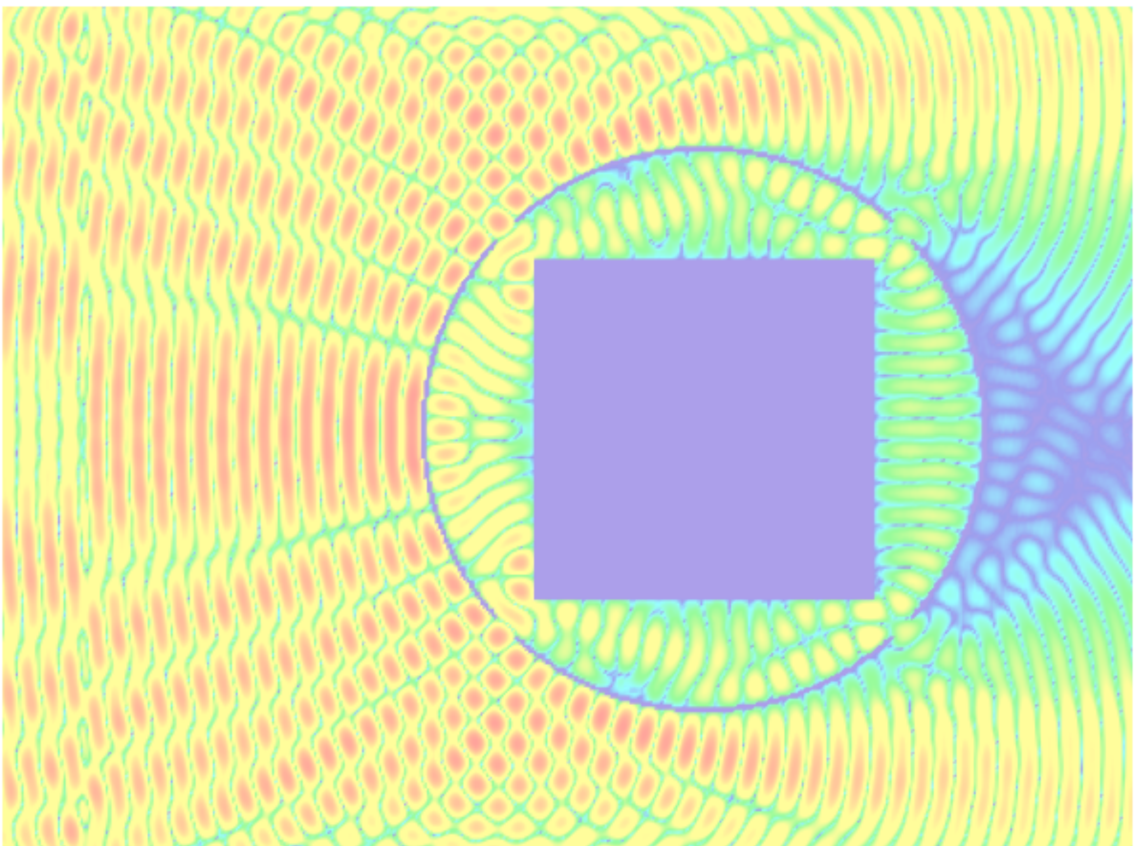

Submitted in Partial Fulfillment of the Requirements for the Masters of Science Degree in Physics

Advisor: Dr. Larry Sorensen

Related to Teaching:

David DeBruyne
Quantum by Example

Armando Lemus
Special Relativity by Example

John Page
Quantum Visualizations with Matlab

Robert Bachilla
Rebecca Adams
Optical Crystals

Diffraction

Optical Crystals and the Seventeen Space Groups

"The goddess of learning is fabled to have sprung full-grown from the brain of Zeus, but it is seldom that a scientific conception is born in its final form, or owns a single parent."
–George Thompson, Nobel Lecture, 1938

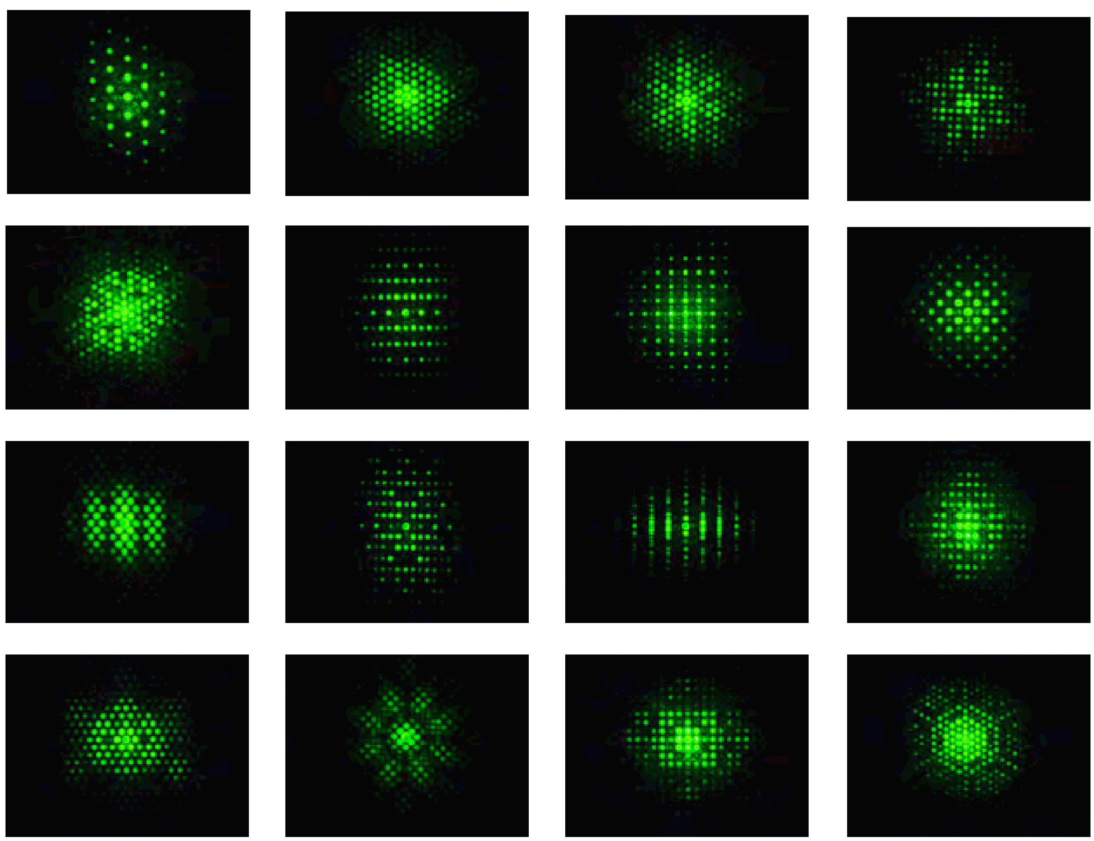

Robert Bachilla

r_bachilla@hotmail.com

Evening Physics Masters Project

Advisor: Dr. Larry Sorensen

University of Washington

December 12, 2006

Related to EMSP Lab Classes:

LabView Control and Analysis
Michael Beard

The Lamb Shift
Larry Brandt

The EPR experiment
Gary Weber
Nicole Gillespie

Surface Plasmon Resonance
Jeremy Cooper
Jin Li

Chaos in Oscillators
Tareq Alrefae
Christopher Cross

Surface Plasmon Resonance

Jeremy Cooper

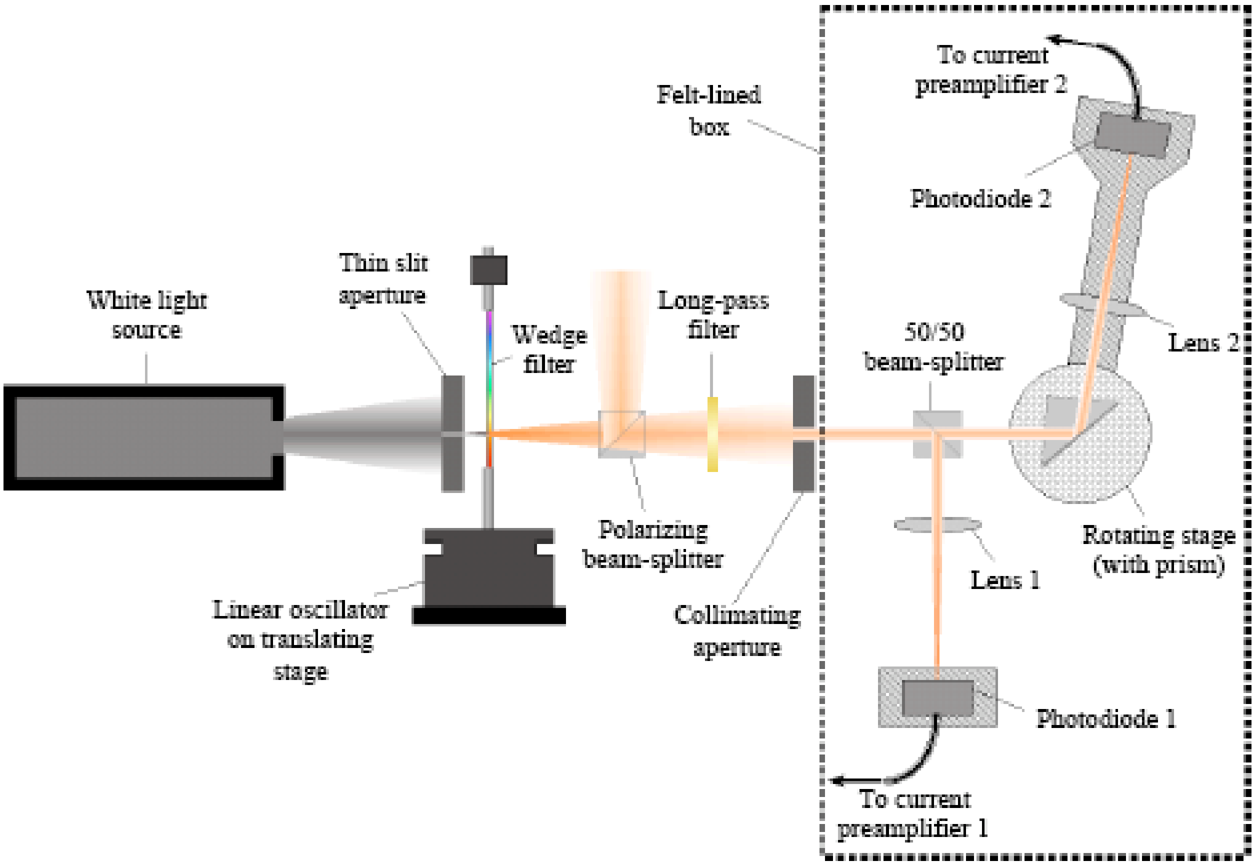

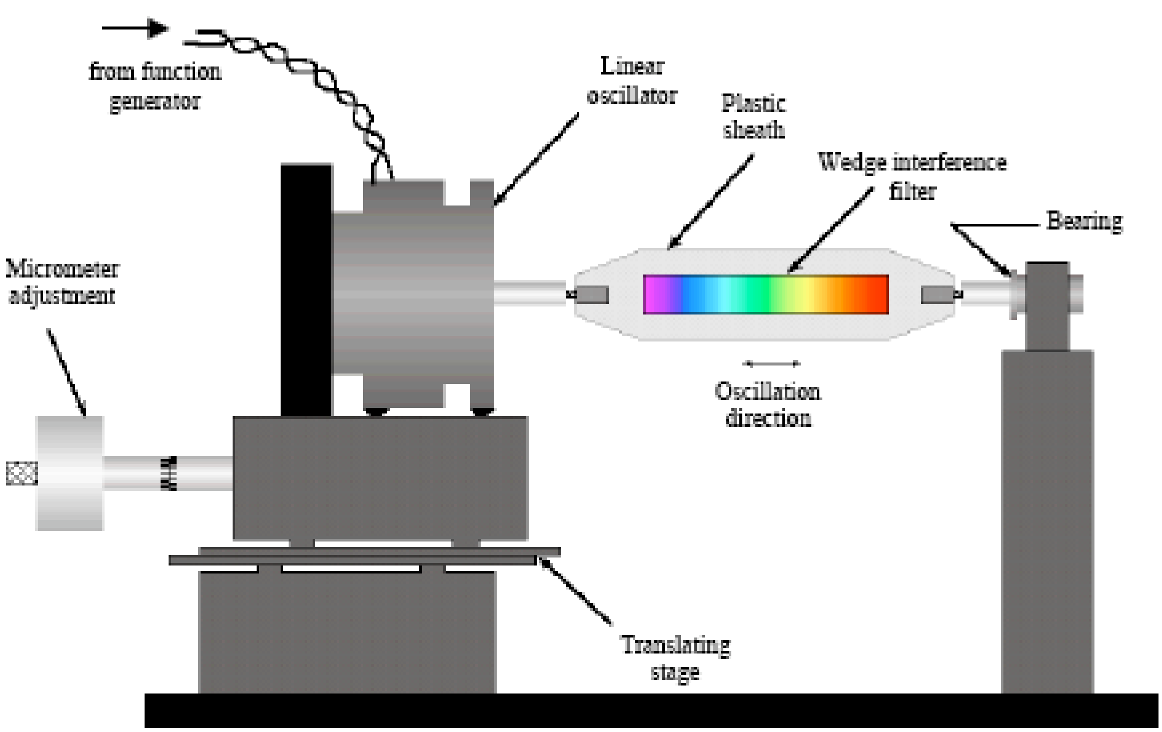

Linear Motion

Wide-Bandwidth Optical Setup
(Felt-lined box removed for clarity)

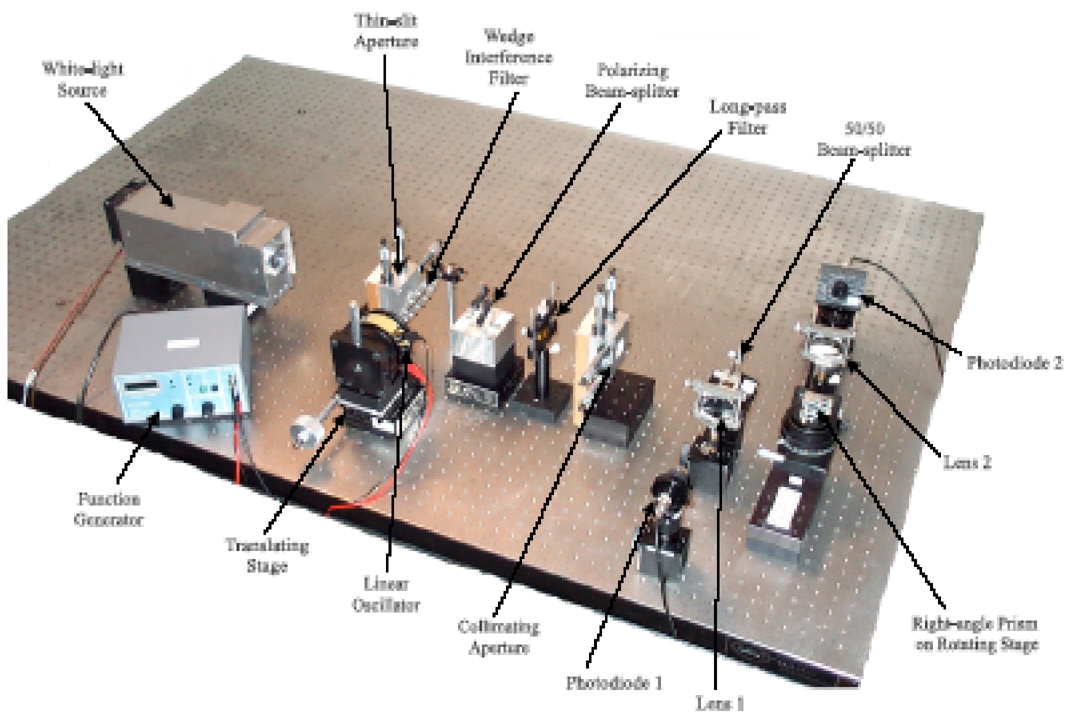

Rotary Motion

Medium-Bandwidth Optical Setup
(Felt-lined box removed for clarity)

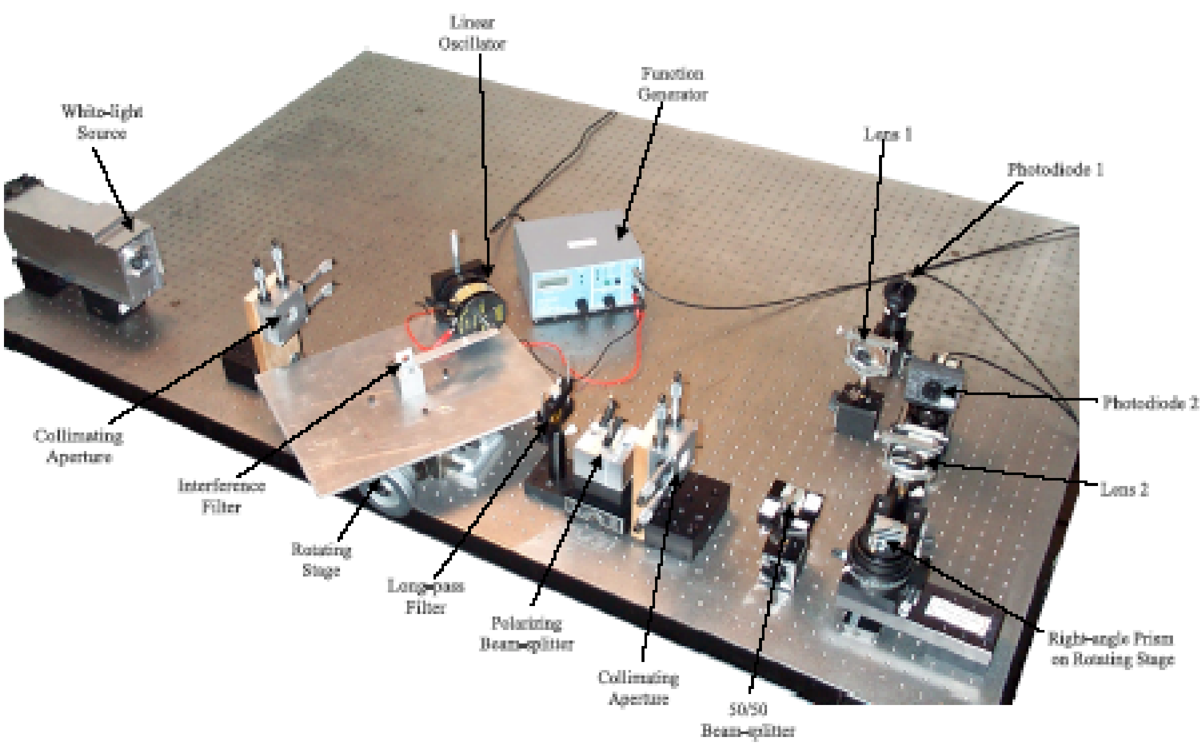

Bifurcations and Chaos in Nonlinear Oscillators

Tareq Alrafae

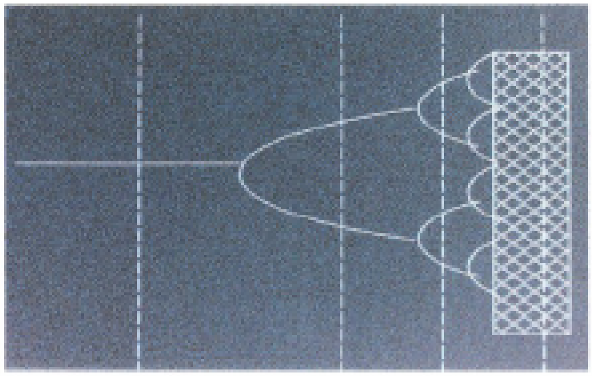

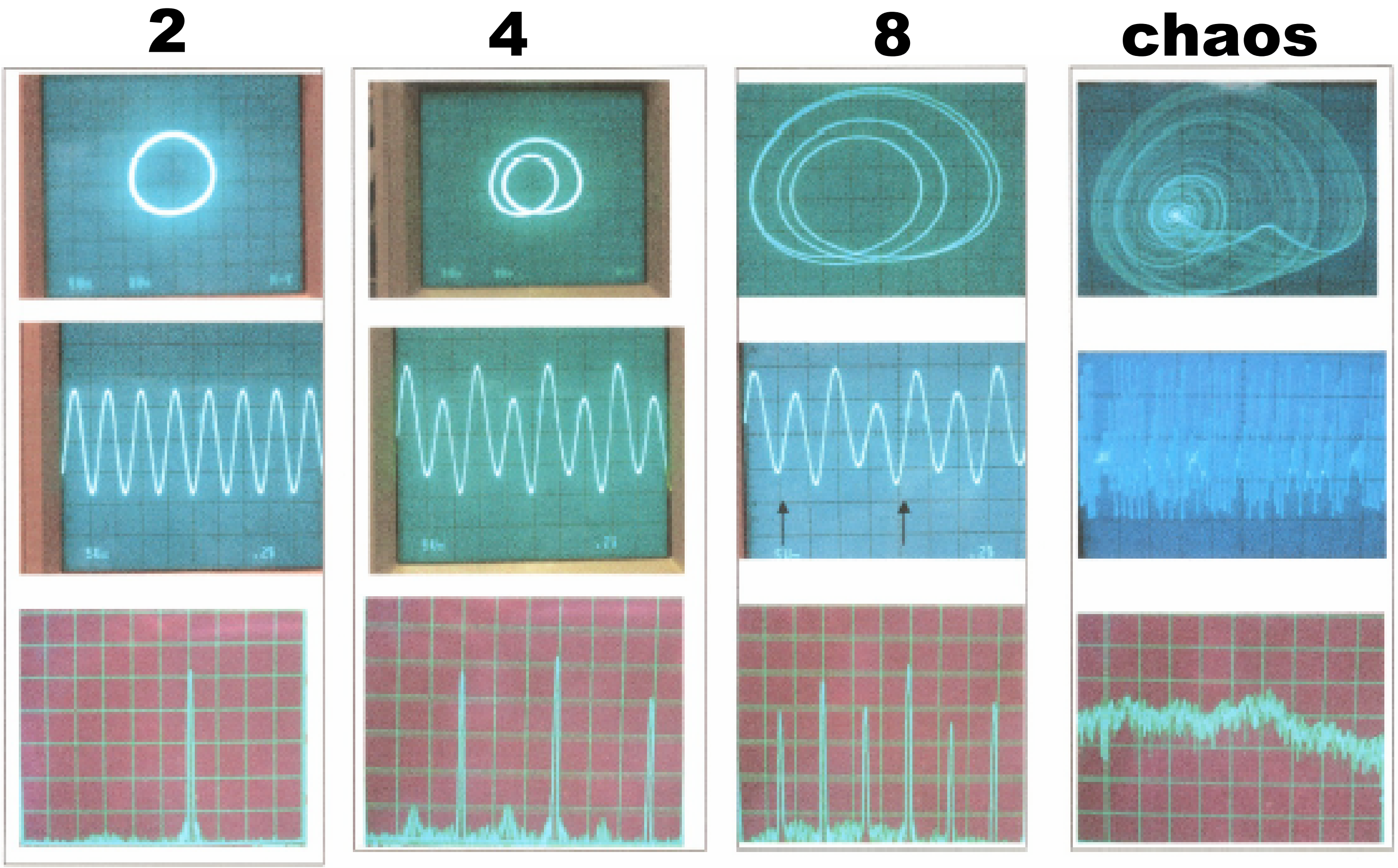

Figures 1a, 1b, and 1c (top to bottom) : phase space, time domain and frequency domain respectively. Period One

Figures 2a, 2b, and 2c (top to bottom) : phase space, time domain and frequency domain respectively. Period Two

Figures 3a, 3b, and 3c (top to bottom) : phase space, time domain and frequency domain respectively. Period Four

Figures 4a, 4b, and 4c (top to bottom) : phase space, time domain and frequency domain respectively. Chaos

With a Medical Physics Group:

Steve Kohlmeyer
Positron Emission Tomography

Joanne Kang
Radiation Therapy

With a Biophysics Group:

Brian Lundstrom
A New Classification of Neurons

Ryan Rule
Image Processing

curves. This behavior is generated by neuronal dynamical systems with fixed points that remain stable regardless of input mean. Thus, these neurons never fire repetitively at steady state in response to noiseless input. We focus in this work on Type B+ neurons whose firing rates are sensitive to input fluctuations throughout the dynamic range and which fire repetitively at steady state to noiseless input.

2D model demonstrating three types of *f-I* curves

We begin with a 2D model, similar to the Hodgkin-Huxley neuron, that can demonstrate three types of *f-I* curves: Type A, B+, and B- (Figure 2). We wish to identify the specific characteristics of the differential equations describing the neuronal dynamics that lead to the generation of Type A vs. B+ behavior. For two-dimensional dynamical systems, these characteristics can be explored geometrically using phase portraits. To do this, we reduced the standard 4D HH model to two dimensions by eliminating the time dependence of m and letting h linearly depend on n (Izhikevich, 2007); we slightly altered the kinetics and conductances. We then examined 2D model trajectories in the phase plane for each of the neuron types.

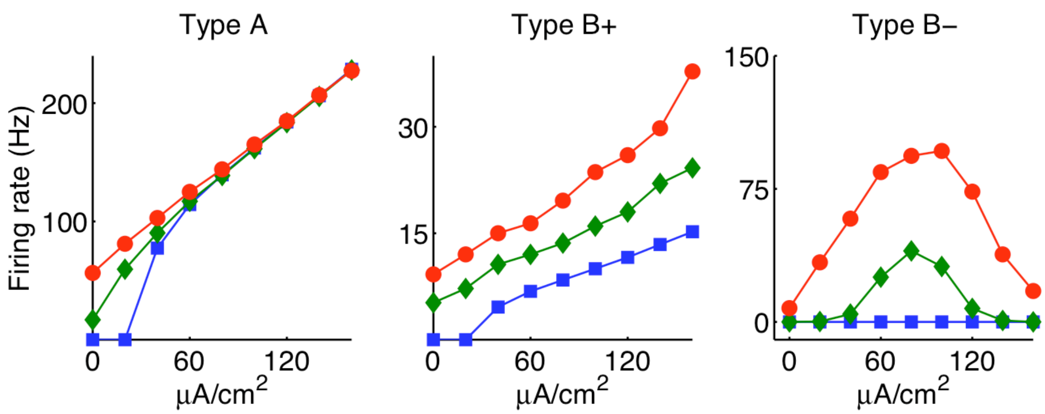

Figure 2: A two-dimensional modified and reduced Hodgkin-Huxley (HH) model neuron can show the three classes of behavior. Type A is similar to the standard HH model and is insensitive to input SD for high currents. In contrast, Type B+ is sensitive to input SD throughout the dynamic range but still fires repetitively to inputs with SD = 0. Type B- models never fire repetitively when input SD = 0 and never undergo a bifurcation from stable fixed point to limit cycle. For the three models, G_{Na} and τ were [50 50 15] mS/cm^2 and [5 100 5] msec, respectively. Other parameters were as given in the Methods section.

Two-dimensional dynamical systems can be analyzed by examining a phase portrait, which is a plot of one dynamical variable against the other (Strogatz, 1994; Gerstner and Kistler, 2002; Izhikevich, 2007). In this case, the model has a "fast" activation variable V and a "slow" inactivation variable n. V is the model's membrane voltage, while n is a combined variable, called the inactivation variable, representing sodium channel inactivation as well as potassium activation. As the membrane voltage V spikes in time, the neuron's trajectory travels counter-clockwise around the phase plane (Figure 3). The upswing and downswing of the action potential (dashed lines) correspond to the left-to-right and right-to-left trajectory jumps, respectively, between the V-nullcline (curvy, solid line). The V-nullcline and n-nullcline (straight, solid line) correspond to points on the phase plane where $dV/dt = 0$ and $dn/dt = 0$, respectively.

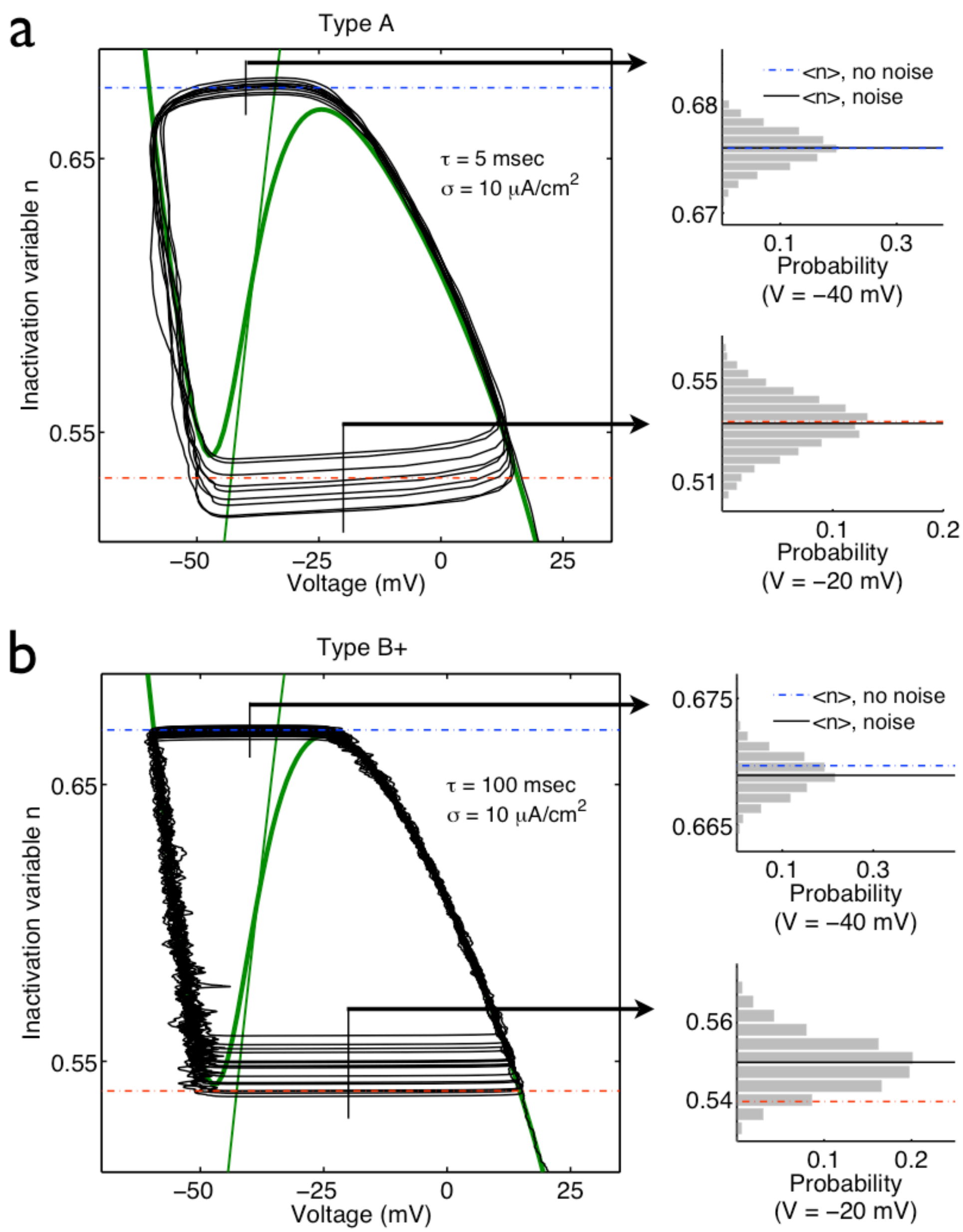

Figure 5: Input fluctuations do not change the mean firing rate when τ is small, but increase firing rate when τ is large. (a) When τ is small (5 msec), input fluctuations ($SD = 10$ μA/cm^2) increase the variance of n during the up- and downswings of the action potential, but do not alter the mean value of n. Histograms are shown at right during action potential upswing ($V = -20$ mV) and downswing ($V= -40$ mV), as indicated by the vertical black lines on the phase portraits. The dashed lines represent the value of n when input $SD = 0$ mV, while the solid lines show the mean values of the data. The dashed and solid lines are nearly the same; the neuron's firing rate does not change with increased input SD, but spiking becomes irregular. **(b)** When τ is large (100 msec), increasing input SD leads to an increasing mean firing rate. Although the mean value of n during the action potential downswing does not appreciably change, during the upswing $\langle n \rangle$ increases, since on average the input SD causes the neuron to spike sooner, i.e. before n has returned to the minimum. The input current I had a mean of 100 μA/cm^2.

Defining an effective potential barrier

Since noise causes the trajectory to jump across the threshold sooner, this implies that there is a barrier that prevents crossing in the absence of noise. To gain insight into how noise drives spiking, we examined how noise-driven trajectories escape over a barrier. Consider a simple 1D model as in Figure 6a, where input fluctuations of typical scale σ cause trajectories to move in the voltage V dimension, such that sometimes the trajectory can overcome an effective potential barrier ΔU located at a threshold for spiking. This picture is reminiscent of problems in physics and chemistry wherein the activation rate is determined by the size of an energy barrier and the temperature and is given by the Arrhenius rate equation, $r \sim \exp(-\Delta U/kT)$. In our case, thermal energy kT is replaced by a factor proportional to the variance of the driving current fluctuations, σ^2.

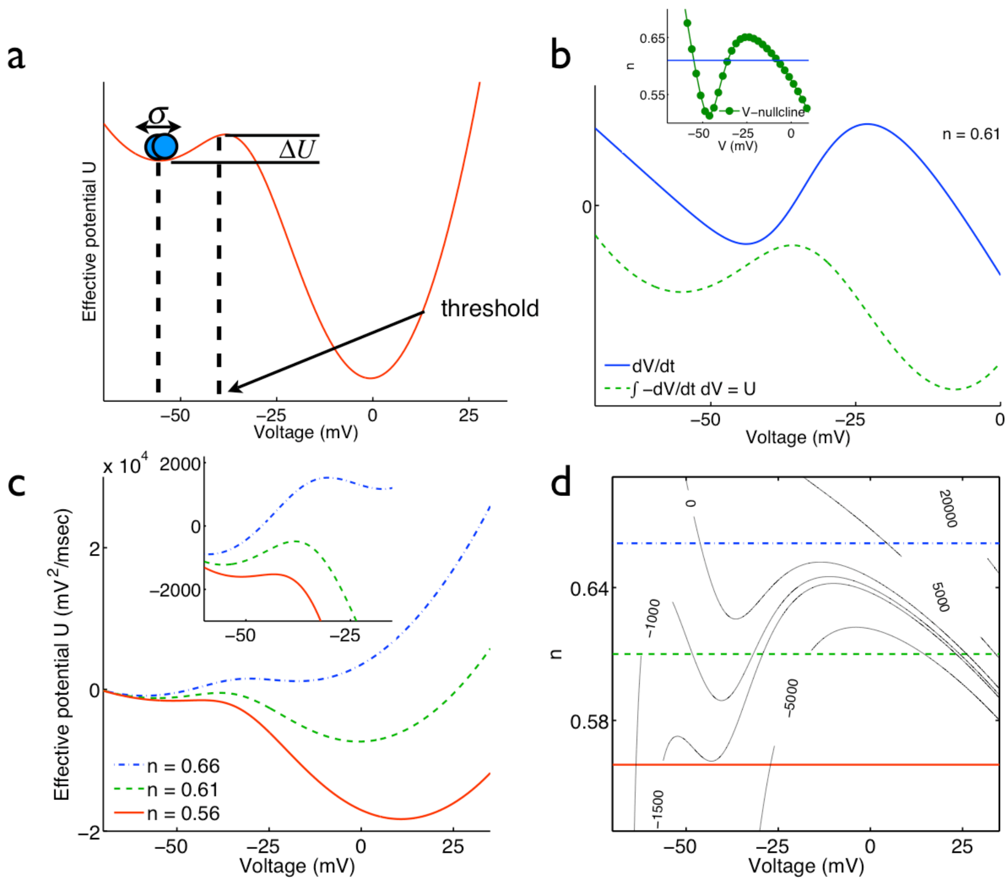

Figure 6: Input fluctuations can shorten interspike intervals by causing the neuron's trajectory to cross an effective potential barrier. (a) A simple 1D model relates spike initiation to crossing an energy barrier and suggests an exponential relation between barrier height and the inactivation time constant for a given level of input fluctuations. **(b)** An effective potential landscape can be found by integrating dV/dt (solid, blue line) with respect to V for constant n. The result of the integral is represented by the dashed, green line. **(c)** The effective potential landscape changes as n changes, and potentials are shown for three specific values of n, which represent three different slices through the inset of **(b)**. The action potential upswing and downswing occur at approximately $n = 0.56$ and $n = 0.66$, respectively. The middle hump is the barrier related to the spiking threshold. Units are defined up

With an Astronomy Research Group:

Nikhil Joshi
Discovering new stars

Tom Erchul
The Black Hole at the Center of our Galaxy

Purely Curiosity Driven:

Virtual Photons and the Aharonov-Bohm Effect

Dev Sen

Feynman Sprinklers

David Wine

Richard Denny

Backyard Tokamak Design

Charles Rust

Quantum Computing

Tad Lisman

Roger Wolfson

A Phenomenological Interpretation of the Aharonov-Bohm Effect in terms of Virtual Photon Exchange by Dev Sen

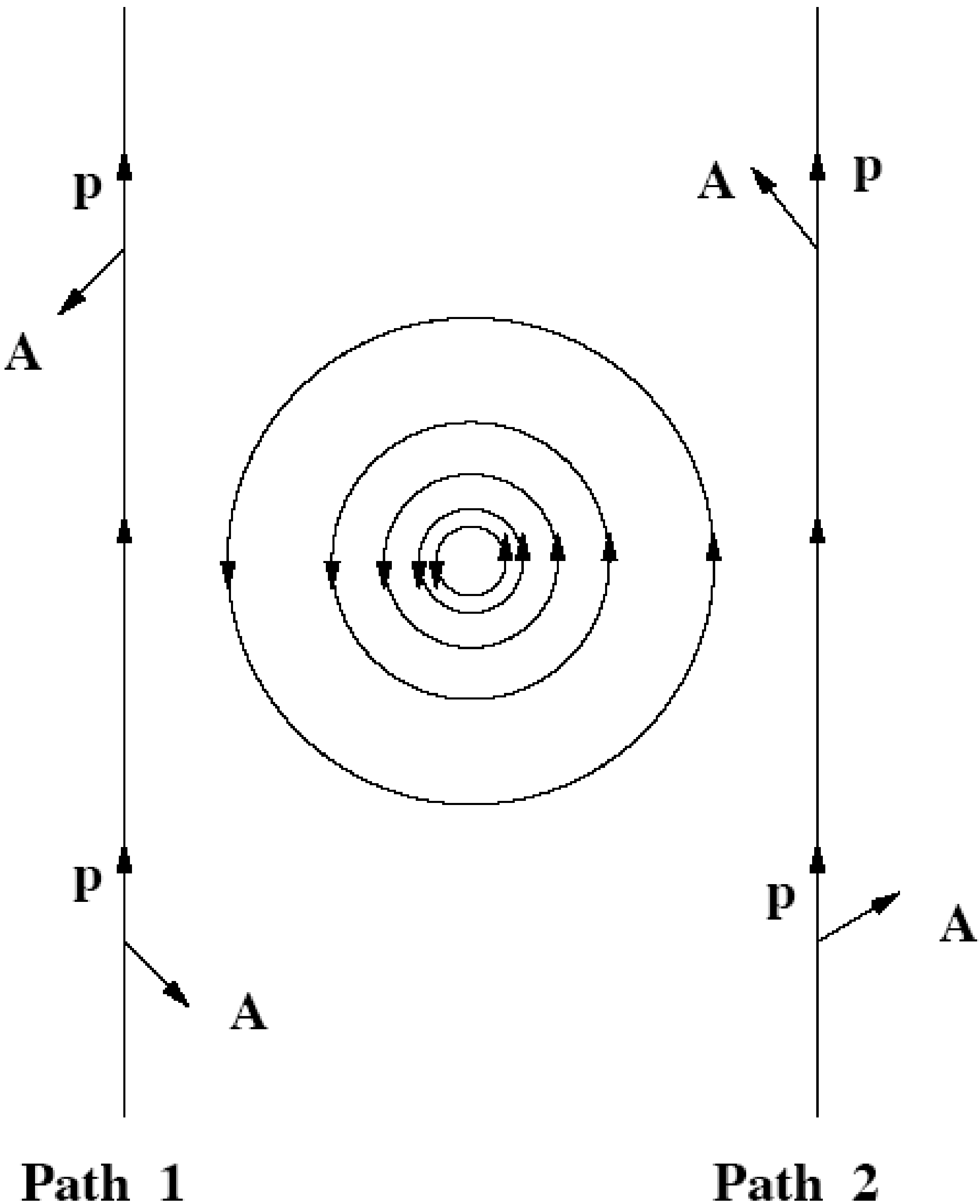

The Feynman Sprinkler Problem

David Wine

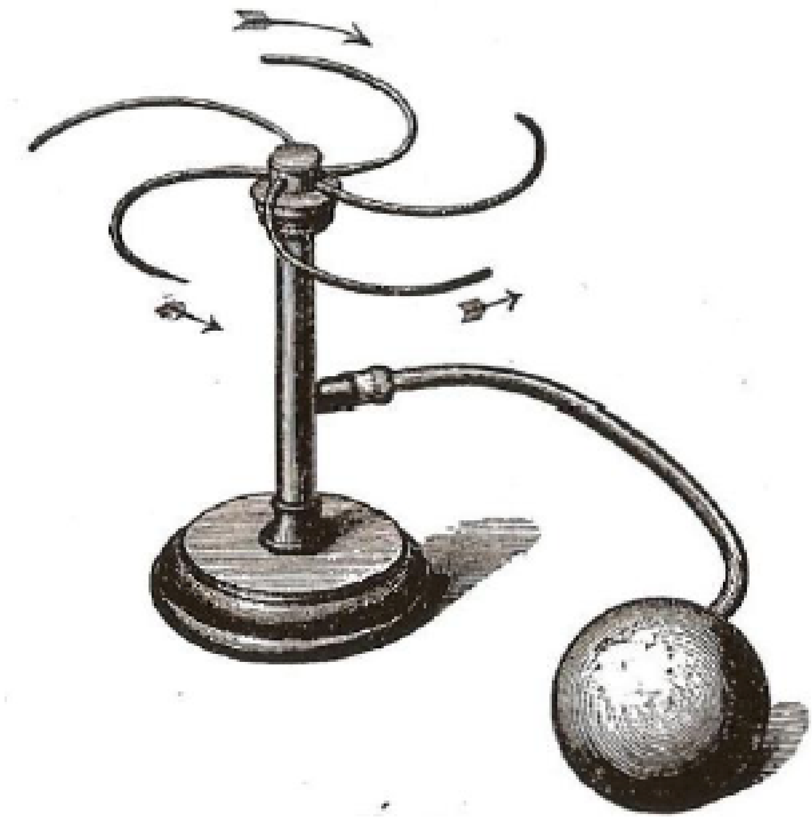

Ernst Mach
Mechanik 1883

Which way will the inverse sprinkler turn?

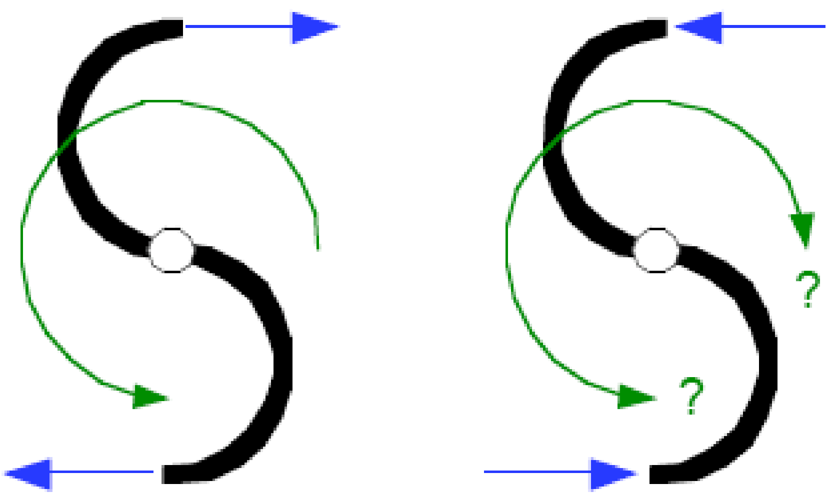

'Forward' 'Inverse'

Richard
Feynman

Richard Denny's Feynman Sprinkler

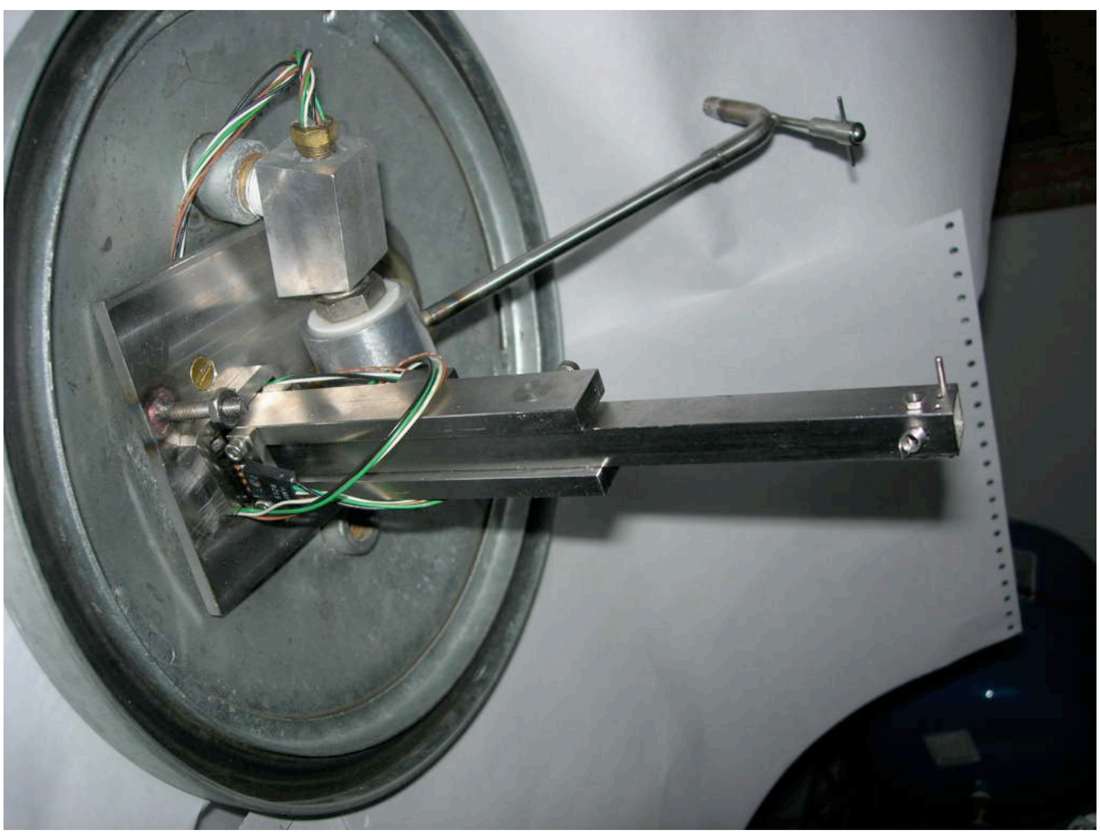

Conceptual Design of a

Small Scale Tokamak Fusion Reactor

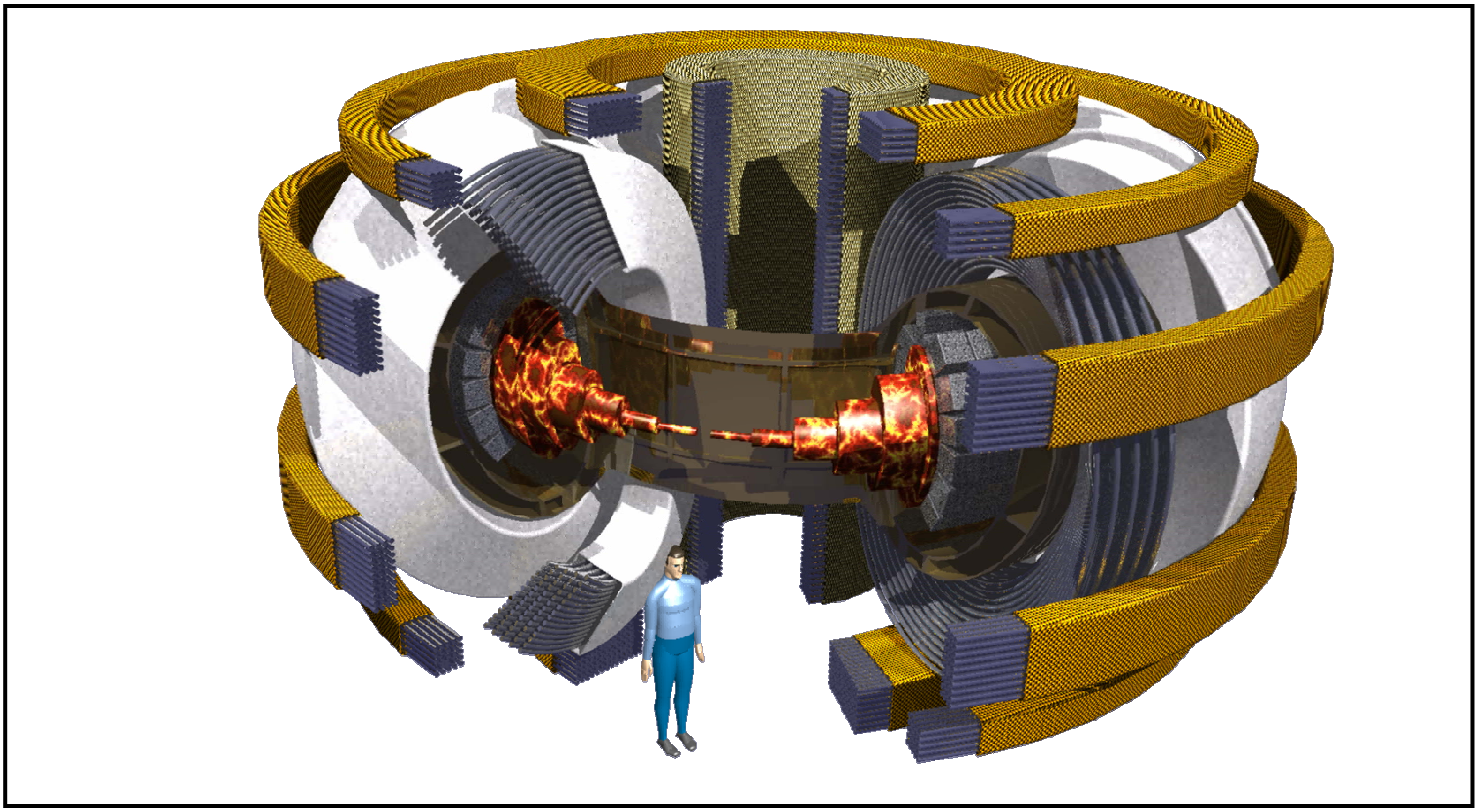

by

Charles Rust

Submitted in partial fulfillment of a Masters Degree of Physics

A Survey of Quantum Computing Algorithms

Tad Lisman

•Hadamard transform

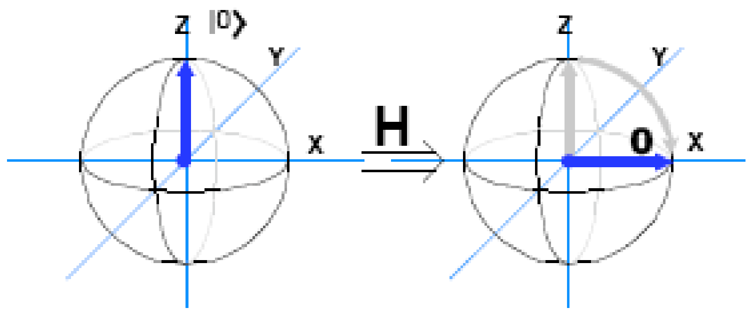

$$H|0\rangle = \frac{1}{\sqrt{2}}\left(|0\rangle + |1\rangle\right)$$

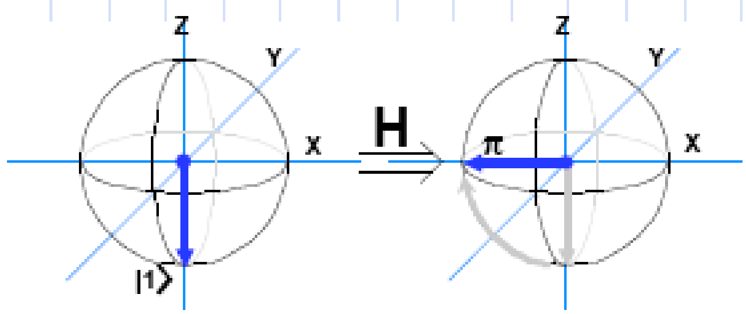

$$H|1\rangle = \frac{1}{\sqrt{2}}\left(|0\rangle - |1\rangle\right)$$

Changes “bit” information to phase information…and phase information back to the “bit” information.

‘These “bras” and “kets”—they’re just vectors! Newly enlightened computer scientist’

“From Cbits to Qbits: Teaching Computer Scientists Quantum Mechanics”
by N. David Mermin AJP 71, 23 (2003)

Related to my research:

Brain Physics

Your Name Here?

Magnetic Memory

Arne Biermans

Jeremy Brockman

Justin Ryser

Paul Unwin

Thomas Montague

X-Ray Holography

John Sinon

Eric Herrera

Roland Mueller

Current carrying wire in a ferrofluid

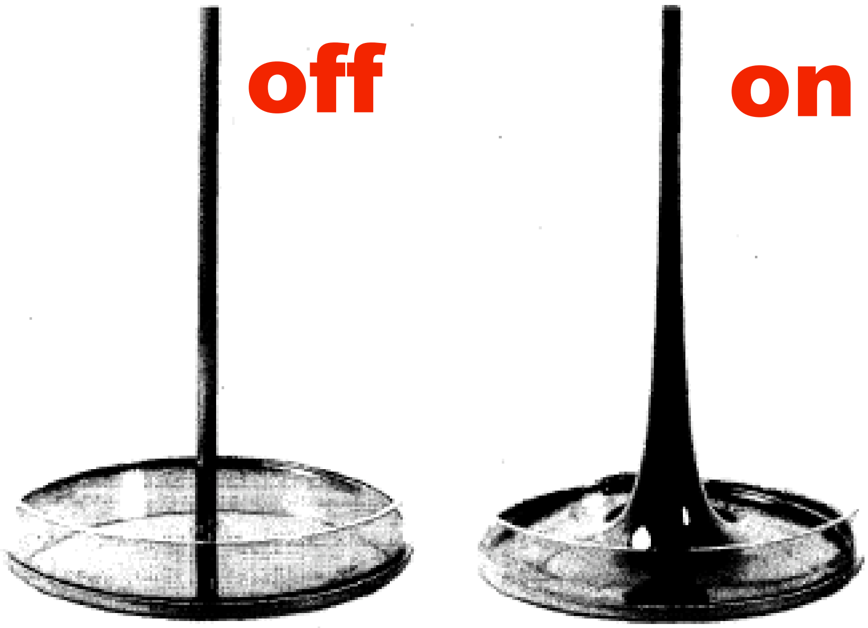

Field applied perpendicular to the surface => ferrofluid kisses

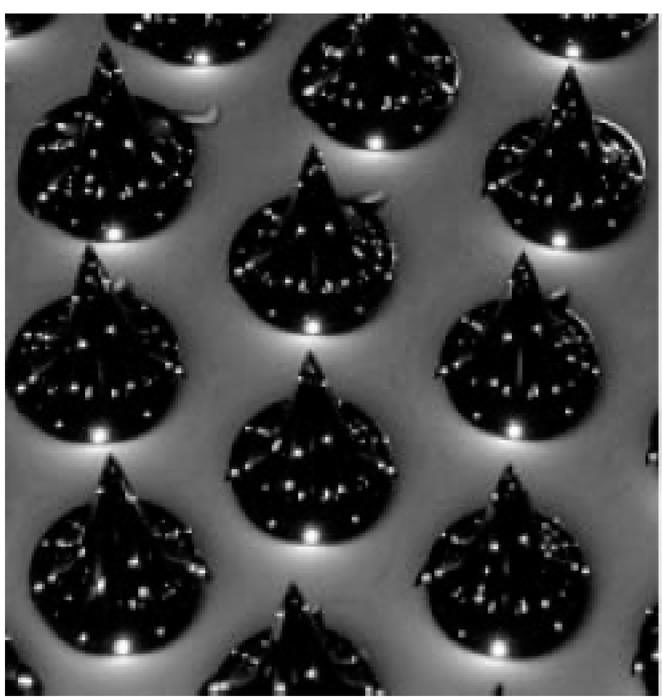

Magnetism versus Gravity

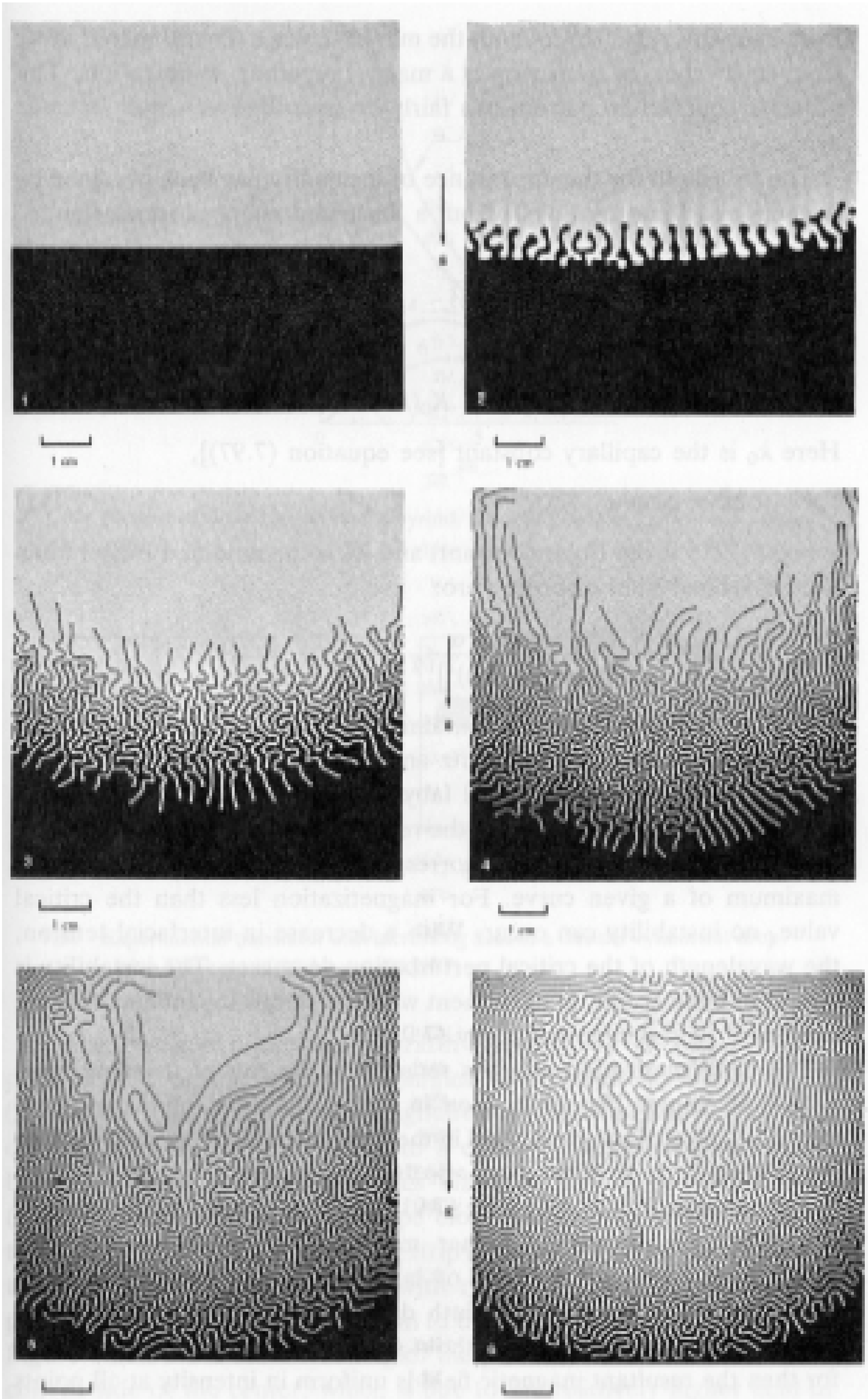

Labyrinths are Ubiquitous

superconductor

vesicle

c

ferromagnetic garnet

ferrofluid

c

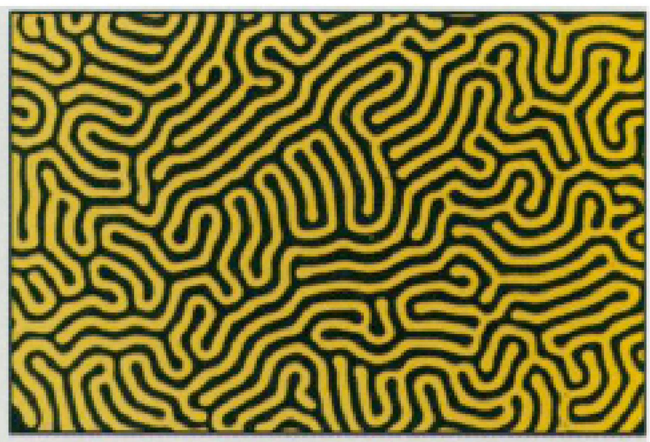

Langmuir monolayer

block copolymer

c

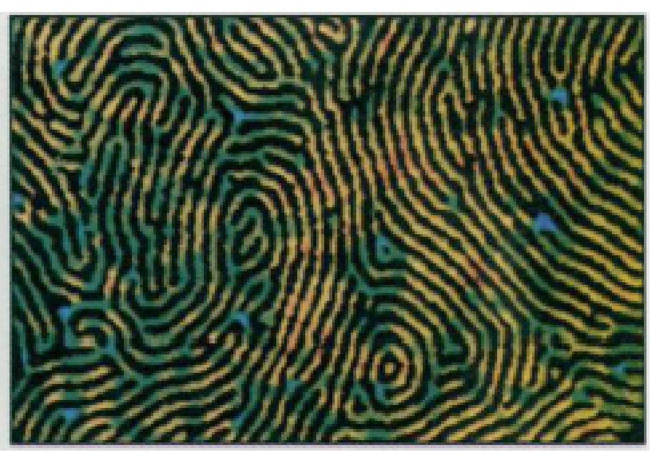

Magnetic Memory in Ferrofluid Labyrinths

Arne Biermans

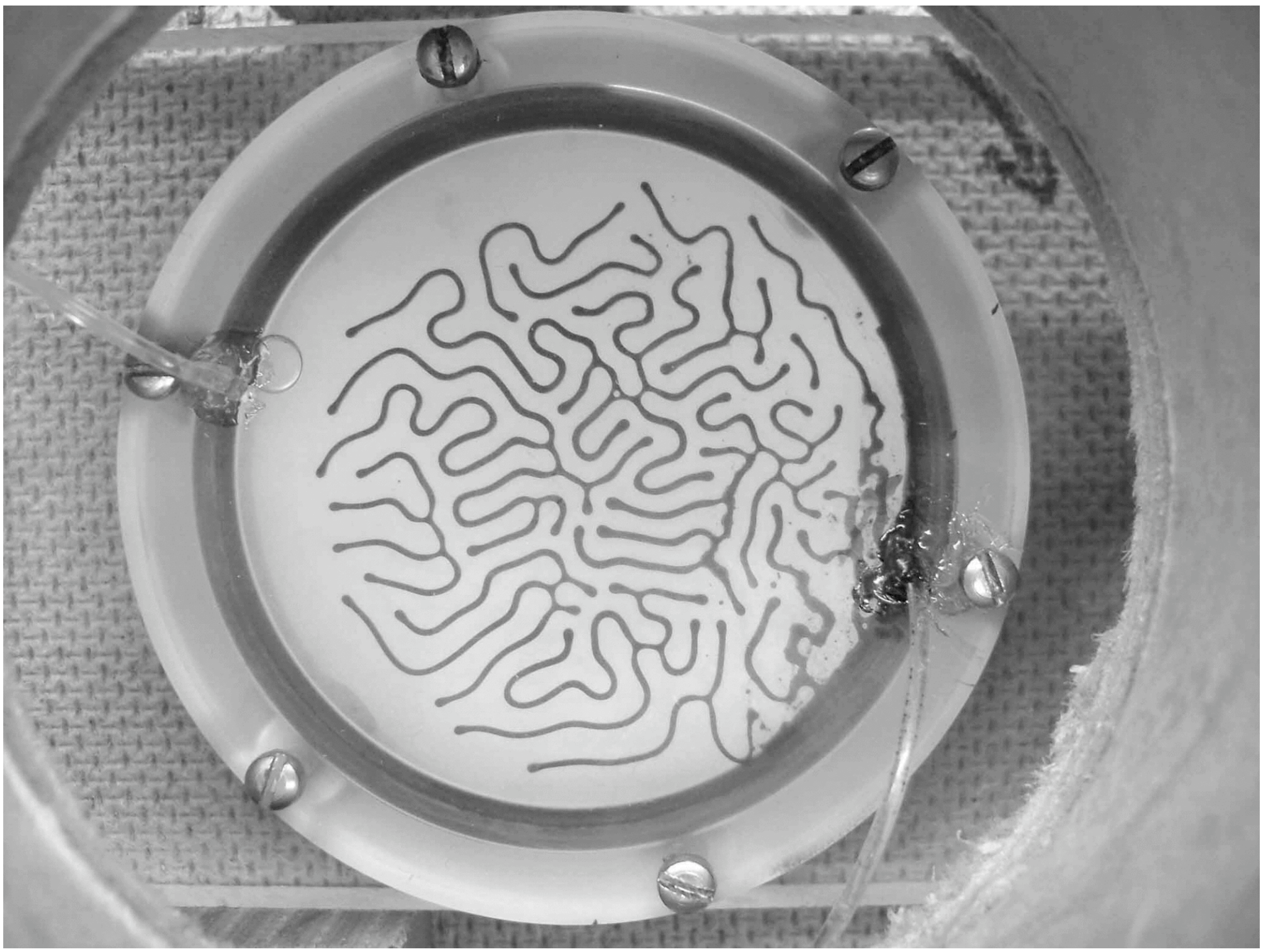

Arne's Movie

Effect of Interfacial Tension on Ferrofluid Labyrinth Formation

Jeremy Brockman

A paper submitted in partial fulfillment of
the requirements for the degree of

Master of Science in Physics

University of Washington

2007

Continued Expansion Results

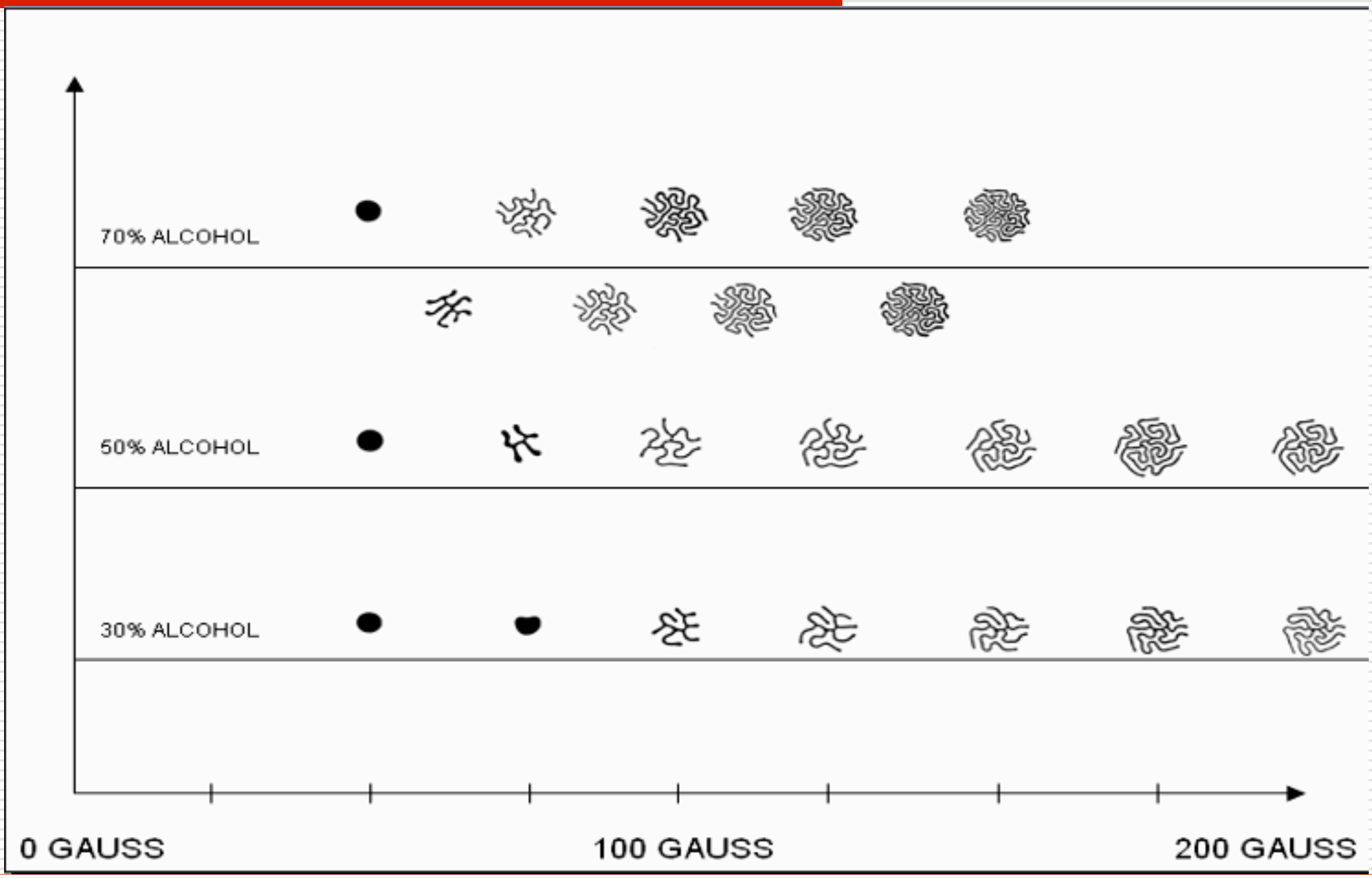

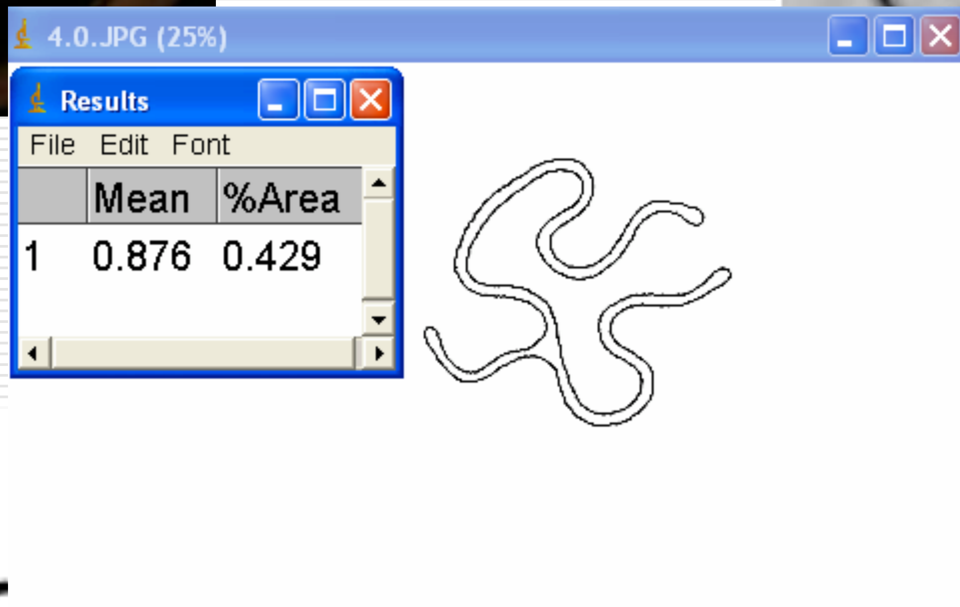
4.0.JPG (25%)
Results
File Edit Font
Mean %Area
1 0.876 0.429

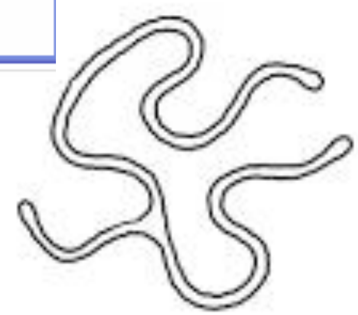

Inside the Magnetic Hysteresis Loop

Paul Unwin

Soft Magnet +Disorder = Hard Magnet

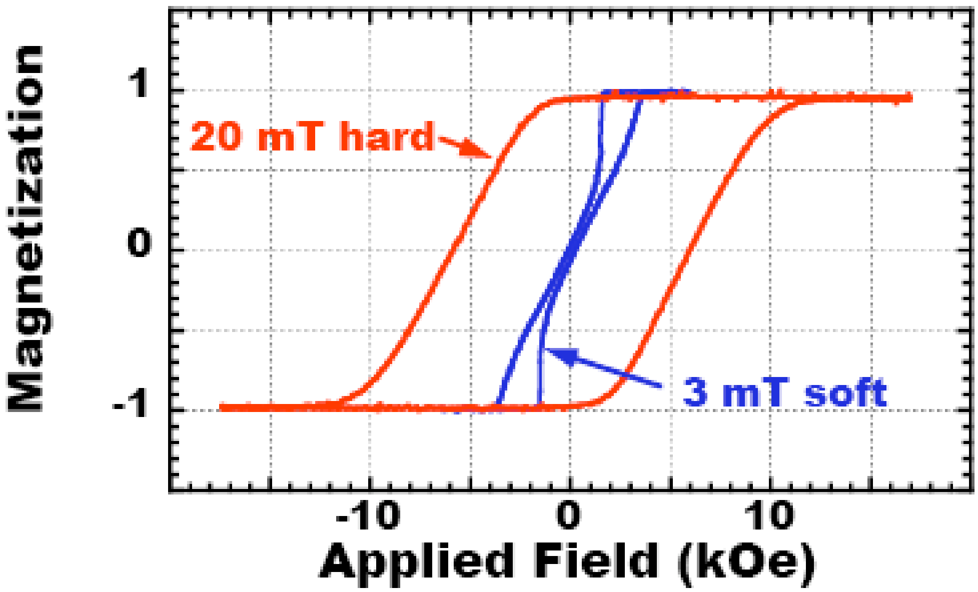

Inside the loop

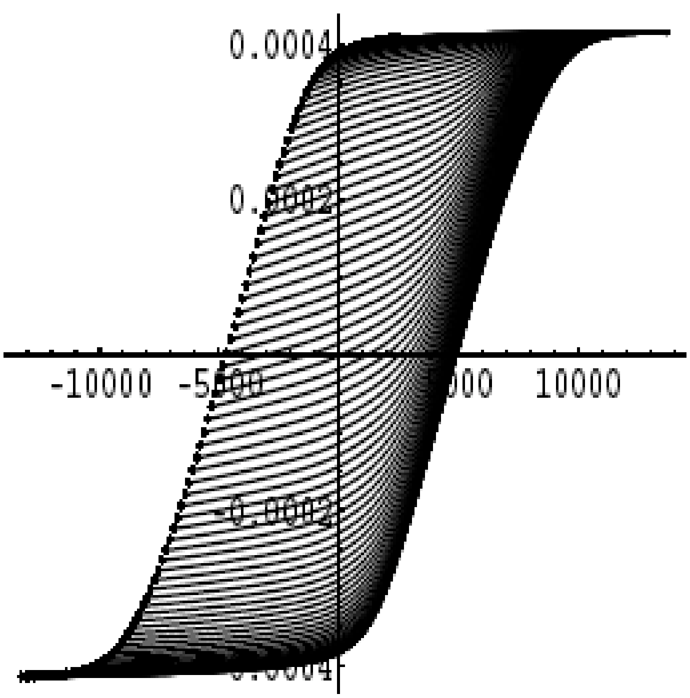

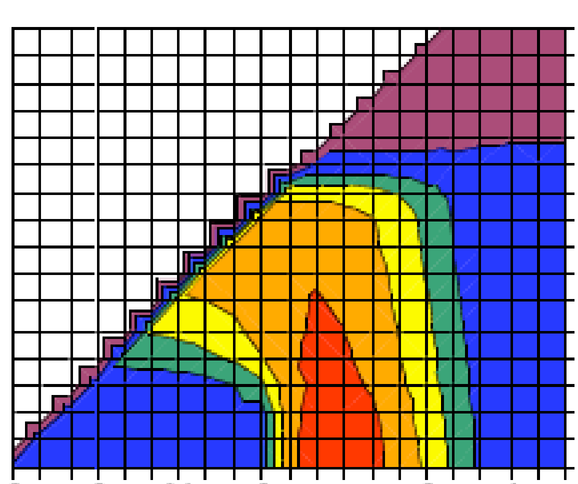

Jim Sethna's Computer Model

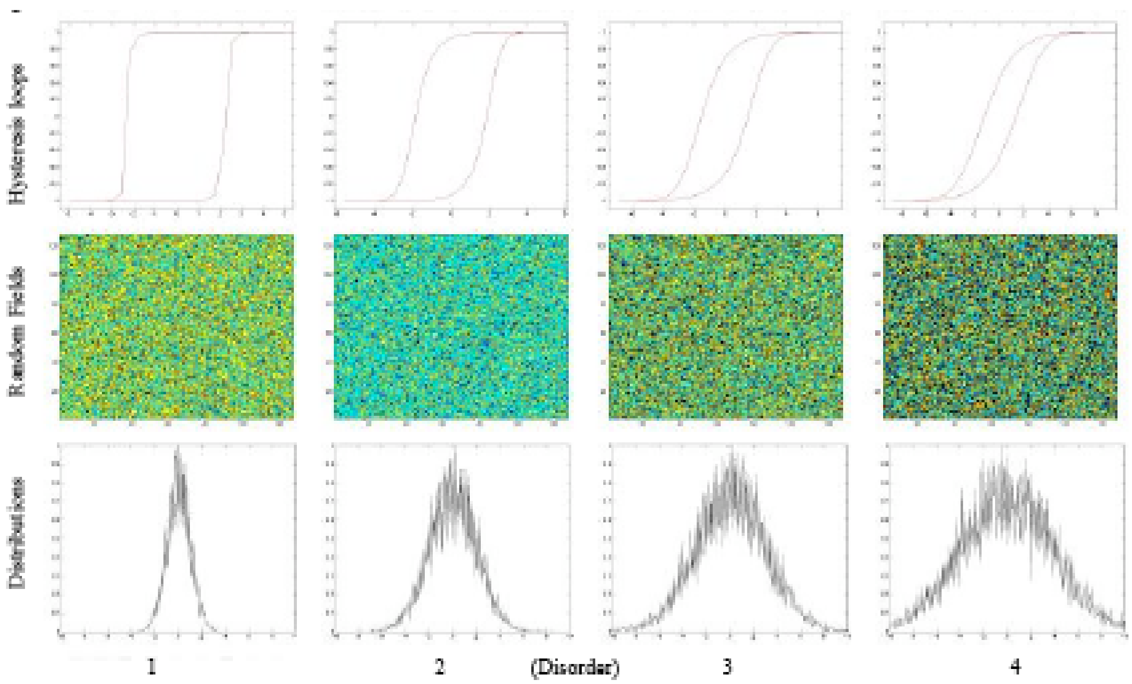

Justin Ryser's Computer Model

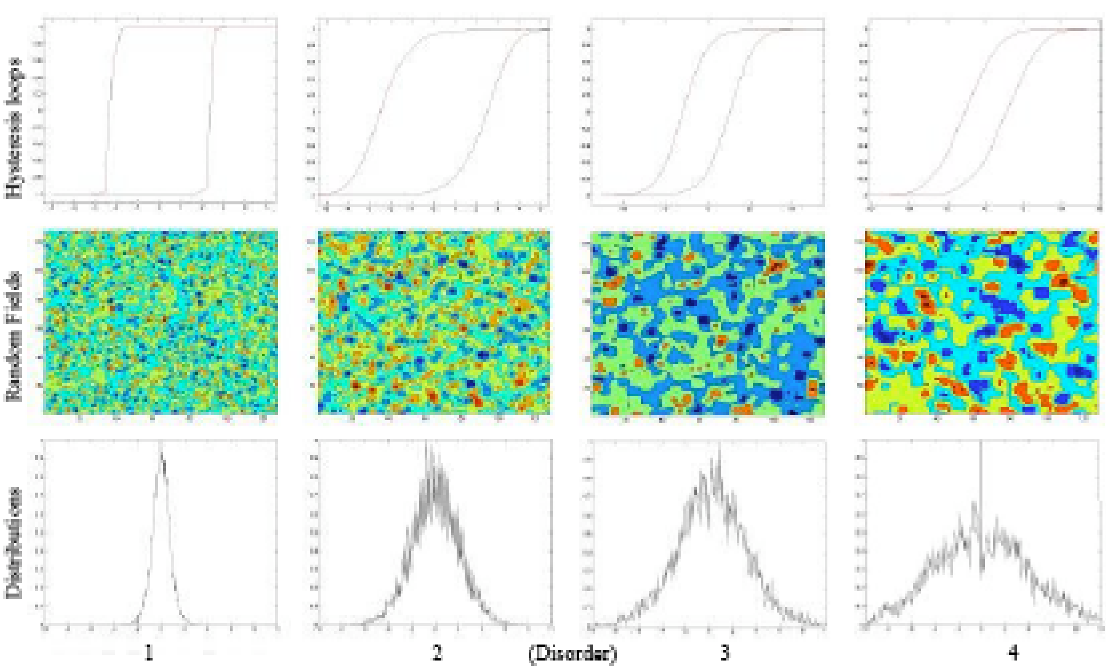

Disorder: Random Fields